a process supported by multiple proteasome-dedicated chaperones such as PAC1-4 and UMP1/POMP in mammals and Pba1-4 and Ump1 in yeast (Kusmierczyk and Hochstrasser, 2008; Murata et al., 2009; Ramos and Dohmen, 2008; Rosenzweig and Glickman, 2008). In contrast to the considerable information on the assembly mechanism and structure of the CP, little is known about the arrangement and assembly of the RP (Murata et al., 2009). However, some extrinsic molecules that associate with certain subunits of the base subcomplex have been identified in mammalian cells, including p28, S5b, and p27.

p28, also known as gankyrin, is a 25 kDa protein of 266 amino acids with six ankyrin repeats that was originally discovered as a subunit of the RP (Hori et al., 1998). Subsequent studies indicated that p28 and its yeast homolog Nas6 are not authentic RP subunits; rather, p28/Nas6 is one of the proteasome-interacting proteins that associates with the RP transiently (Dawson et al., 2002; Verma et al., 2000; Wang et al., 2007). p28 was reported to interact with Rpt3 in the RP, not in the 26S proteasome (Dawson et al., 2002; Nakamura et al., 2007). At the same time, it has been reported that p28 binds to MDM2 ubiquitin ligase and enhances the degradation of two important tumor suppressors, pRb and p53, presumably by recruiting these molecules in the vicinity of the proteasome, thus suggesting an oncogenic potential of p28 (Dawson et al., 2006; Higashitsuji et al., 2000).

S5b, a 56 kDa protein of 504 amino acids, was initially identified as a component of the 26S proteasome purified from human red blood cells (Deveraux et al., 1995). It forms a tetramer with Rpt1, Rpt2, and Rpn1 in vitro (Richmond et al., 1997), but its function in the proteasome is totally unknown. Like p28, it is reasonable to regard S5b as a proteasome-interacting protein since it was not found or was detected only in small amounts compared with the integral subunits in proteomics analyses of mammalian 26S proteasomes (Gomes et al., 2006; Wang et al., 2007).

p27, a 25 kDa protein of 223 amino acids, was discovered as a component of a PA700-dependent activator with a molecular mass of approximately 300 kDa that is also known as "the modulator" (DeMartino et al., 1996). The modulator complex is composed of p27, Rpt4, and Rpt5 and is considered to enhance the association between the RP and the CP (Adams et al., 1997), although the mechanism is unidentified.

In this study, beginning with proteomics analysis, we characterized the above three proteasomal ATPase-interacting proteins in mammalian cells. The combination of small interfering RNA (siRNA)-mediated knockdown and biochemical approaches uncovered their roles as molecular chaperones that regulate the assembly of the base subcomplex of the mammalian proteasome.

RESULTS

p28, S5b, and p27 Are Proteasome-Dedicated Molecules in HEK293 Cells

Although originally identified as proteasome-associated proteins, the functional relevance of p28, S5b, and p27 to the proteasome is poorly understood. Since deletion of *Nas6* and *Nas2*, yeast orthologs of mammalian p28 and p27, respectively, did not result in any obvious defect in proteasome function at least under normal conditions (Dawson et al., 2002; Hori et al., 1998; Watanabe et al., 1998), we wondered whether these molecules are really involved in some functions of the proteasome. To gain insights into their roles, we explored molecules that physically interact with these proteins in mammalian cells. Flag-tagged p28, S5b, and p27 were expressed in HEK293 cells, and anti-Flag immunoprecipitates were analyzed by liquid chromatography coupled with tandem mass spectrometry (Natsume et al., 2002). Proteins that are associated with UCH37, a well-established proteasome-interacting protein (Hamazaki et al., 2006; Jorgensen et al., 2006; Qiu et al., 2006; Wang and Huang, 2008; Yao et al., 2006), were also analyzed. UCH37 precipitated all subsets of proteasome subunits, including subunits of the CP and the RP, illustrating that it plays a role in the context of the 26S proteasome (Table S1 available online). We also found that p28, S5b, and p27 predominantly coprecipitated proteasome subunits, suggesting that these molecules are basically specialized for proteasomes (Table S1). However, unlike UCH37, they precipitated only a restricted subset of the proteasome subunits. p28 with C-terminal Flag tag and S5b almost exclusively coprecipitated the RP subunits but did not coprecipitate any of the CP subunits. Furthermore, p28 with an N-terminal tag pulled down only two specific ATPase subunits,Rpt3 and Rpt6, together with PAAF1 (proteasomal ATPase-associated factor 1), which is likely the human homolog of the yeast Rpn14 (hereafter we refer to it as Rpn14) and has been reported to associate with certain ATPase subunits of the base and to inhibit RP-CP interactions when overexpressed in HeLa cells (Park et al., 2005). p27 also precipitated specifically Rpt4 and Rpt5, irrespective of the tag position. These findings suggest that these three molecules play their roles in the context of the RP, and more specifically, the base subcomplex with respect to p28 and p27.

Three Distinct Modules Containing Specific Base Subunits and the Associating Proteins In Vivo

To examine the size distribution of p28, S5b, and p27, we separated extracts from HEK293T cells by 8%–32% glycerol gradient centrifugation. None of the three molecules nor Rpn14 was detected in the 26S proteasome fraction (Figure 1A, fraction 26), consistent with the results of mass spectrometric analysis (Table S1). Rather, they were distributed in the light fractions, where small portions of the base subunits were also distributed (Figure 1A, fractions 4–12).

To test whether p28, S5b, and p27 are associated with proteasome subunits in these light fractions, we subjected extracts from cells stably expressing Flag-tagged p28, S5b, or p27 to fractionation by low-density (4%–24%) glycerol gradient centrifugation to better resolve the light fractions. The distribution patterns of exogenously expressed p28, S5b, and p27 were essentially similar to those of endogenous proteins, ranging from fraction 4 to fraction 16 (Figures 1B–1D; see also below). These fractions were immunoprecipitated with anti-Flag antibody, followed by immunoblotting for proteasome subunits and Rpn14. p28 coprecipitated specifically with Rpt3 and Rpt6 as well as Rpn14 but neither with other base subunits nor with lid subunits in fractions 8–12 (Figure 1B). Although we do not know the exact stoichiometries of p28, Rpn14, Rpt3, and Rpt6

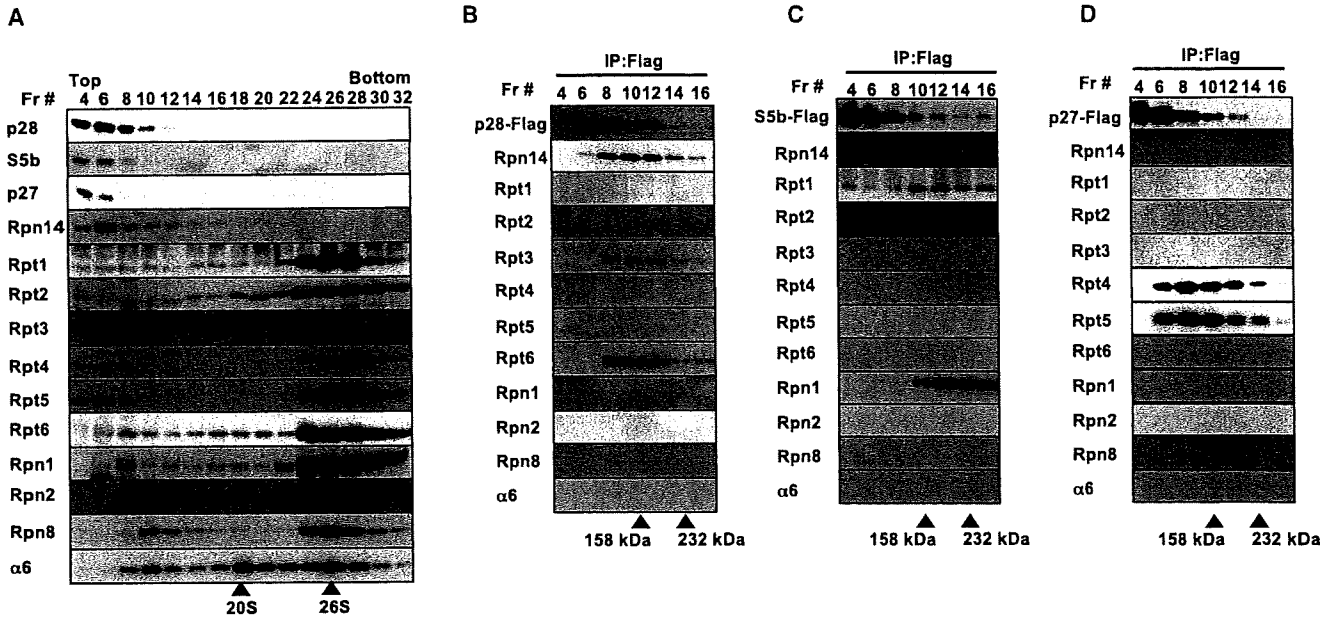

Figure 1. p28, S5b, and p27 Form Distinct Complexes with Specific Base Subunits

(A) Extracts from HEK293T cells were fractionated by 8%–32% glycerol gradient centrifugation, followed by immunoblotting of each fraction with the indicated antibodies. Arrowheads depict the locations of the CP (20S) and 26S proteasome (26S).

(B–D) Extracts from HEK293T cells stably expressing Flag-tagged p28 (B), S5b (C), and p27 (D) were fractionated by 4%–24% glycerol gradient centrifugation. The indicated fractions were immunoprecipitated with M2 agarose and analyzed by SDS-PAGE and immunoblotting. The locations of size markers are depicted.

in this complex or whether some other nonproteasomal factors are associated with this complex, the sedimentation rate matches the deduced size of 160 kDa of the tetrameric complex of p28, Rpn14, Rpt3, and Rpt6, which is supported by the peak location of a 158 kDa size marker at fraction 10. Likewise, S5b formed a complex with Rpt1, Rpt2, and Rpn1 at fractions 12–16, consistent with the heterotetrameric complex of these proteins with its deduced size of 250 kDa as revealed by the peak location of a 232 kDa marker at fraction 13 (Figure 1C). p27 also specifically associated with Rpt4 and Rpt5 with its peak at fraction 8, which is consistent with the trimeric complex formation of p27, Rpt4, and Rpt5, whose deduced size is approximately 120 kDa (Figure 1D). Accordingly, Rpn2 is the only base subunit not included in any of these complexes.

These data indicate that each ATPase subunit of the base subcomplex is paired with a particular ATPase subunit in a combination of Rpt3 and Rpt6, Rpt1 and Rpt2, or Rpt4 and Rpt5, which is further associated with a specific proteasome-dedicated molecule as well as a non-ATPase subunit, p28 and Rpn14, S5b and Rpn1, or p27, respectively. Thus, the base subunits with the exception of Rpn2 form distinct small modules before the formation of the base subcomplexes.

Specific Subunit Interactions within the Modules

To examine protein-protein interactions within the modules, we cotranslated molecules of interest in the presence of [^{35}S] methionine and used the resulting radiolabeled proteins in binding assays. p28 was associated strongly with Rpt3 among the ATPase subunits (Figure 2A, left), while Rpt3 was specifically associated with Rpt6 and vice versa (Figure 2A, two middle panels). Rpn14 interacted most notably with Rpt6 (Figure 2A, right), thus enabling the formation of the p28-Rpt3-Rpt6-Rpn14 complex (the p28 module).

S5b was bound strongly to Rpt1 among the ATPase subunits (Figure 2B, left). Rpt2 appeared to bridge between the Rpt1 and Rpn1 because Rpt2 was directly associated with both Rpt1 and Rpn1 while Rpt1 interacted with Rpt2 (Figure 2B, middle and right), which accounts for the formation of the S5b-Rpt1-Rpt2-Rpn1 complex (the S5b module). On the other hand, p27 directly associated with Rpt5 while Rpt4 and Rpt5 specifically interacted with each other (Figure 2C), resulting in the formation of the p27-Rpt5-Rpt4 complex (the p27 module).

Although we detected several other weak interactions not mentioned above, which may or may not be significant, the above in vitro analyses essentially verify the specific complex formation of the base subunits observed in mammalian cells (Figure 1) and illustrate the basis for the organization of the three modules.

Module Formation Is Important for the Stability of the Base Subunits

To explore the rationale for such specific pair or trio formations of the base subunits, we knocked down each base subunit as well as the lid subunit Rpn3, and the cell extracts were subjected to immunoblot analysis (Figure 3A).

Knockdown of Rpt1, Rpt2, or Rpn1 resulted in reduction in the two other base subunits of the S5b module, although the decrease in Rpn1 was modest compared to those in Rpt1 and Rpt2 in Rpt2- and Rpt1-knockdown cells, respectively. Likewise, knockdown of Rpt3 and Rpt6 led to a decrease in Rpt6 and Rpt3,

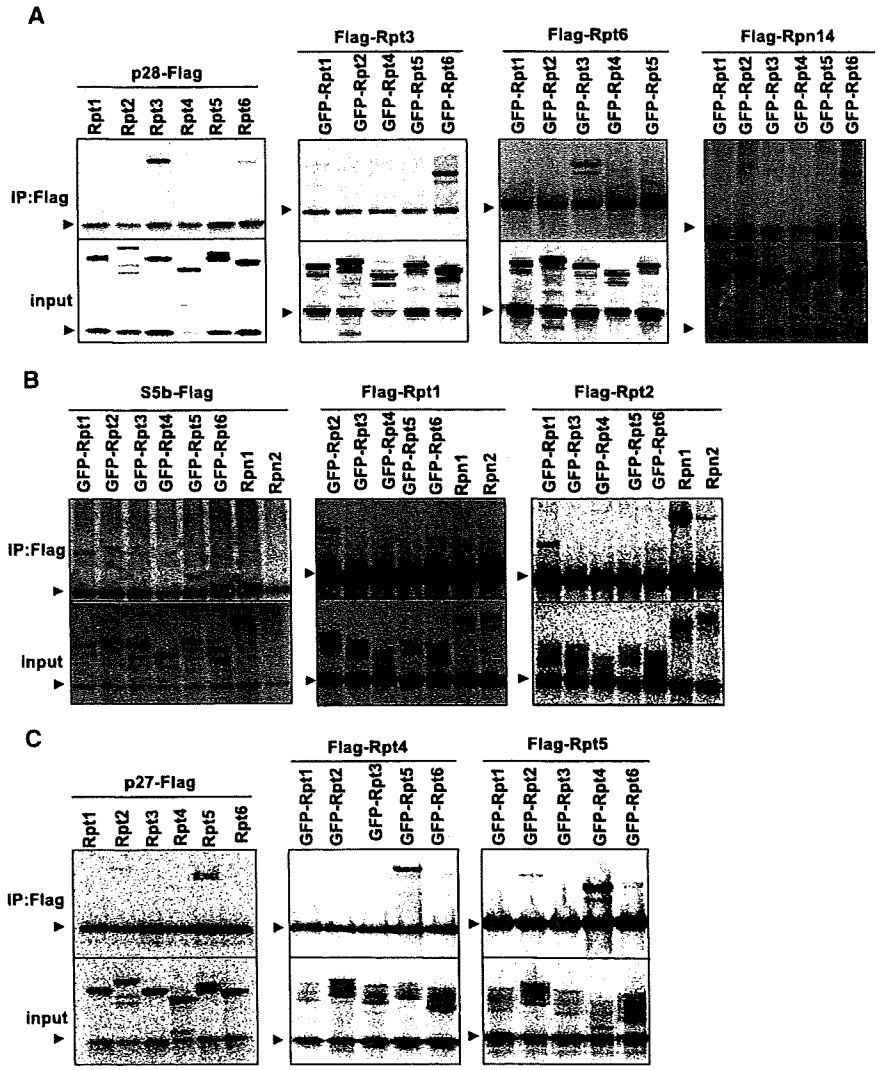

Figure 2. Direct Interaction of p28, S5b, and p27 with Base Subunits

(A) Flag-tagged p28, Rpt3, Rpt6, and Rpn14 were cotranslated and radiolabeled with Rpt subunits, immunoprecipitated with M2 agarose, and analyzed by SDS-PAGE and autoradiography.

(B) Associations of Flag-S5b, -Rpt1, and -Rpt2 with base subunits were analyzed as in (A).

(C) Associations of Flag-p27, -Rpt4, and -Rpt5 with Rpt subunits were analyzed as in (A). Arrowheads indicate Flag-tagged proteins, and other bands are from nontagged or GFP-tagged proteins.

respectively; knockdown of Rpt4 and Rpt5 caused a decrease in Rpt5 and Rpt4, respectively. In these cells, expression levels of mRNA transcripts for the base subunits were not decreased, but rather increased (Figure S1), consistent with the previous observation that proteasome dysfunction activates proteasomal gene expression (Meiners et al., 2003). This suggests decreased protein stabilities of unpaired base subunits.

In contrast, knockdown of Rpn2, which is not included in any of the three modules, did not significantly affect the expression levels of the other base subunits. Knockdown of Rpn3 did not influence the base subunits, including Rpn2, supporting the previous notion that the lid and the base are assembled independently (Isono et al., 2007).

Intriguingly, Rpn10 was decreased in the absence of either base subunits or a lid subunit, suggesting that Rpn10 is stabilized only when both the base and the lid are integral. p28, S5b, and p27 were not affected by loss of the base subunits (Figure 3A).

These data demonstrate that knockdown of a base subunit causes reduction in its partner subunit within the module and suggest that the formation of the modules is necessary for stable expression of the base subunits before the assembly of the base subcomplex, where the presence of the proteasome-dedicated molecules p28, S5b, and p27 is not sufficient for the stability of the base subunits.

Modules Are Assembled En Bloc to Form the Base Subcomplex

To examine the influence of loss of each base subunit in detail, we separated the knockdown lysates shown in Figure 3A by native-PAGE, followed by immunoblotting (Figures 3B–3J).

Knockdown of each of Rpt1, Rpt2 or Rpn1, which caused disruption of the S5b module, exhibited essentially the same phenotype; these cells showed accumulation of complexes of similar size that included subunits of the other two intact modules, i.e., Rpt3, Rpt4, Rpt5, and Rpt6 (Figures 3D–3G). Knockdown of Rpt3 and Rpt6, subunits of the p28 module, also resulted in accumulation of a complex of similar size and similar subunit composition that included Rpt1, Rpt2, Rpn1, Rpt4, and Rpt5, which are the subunits of the other two modules (Figures 3B, 3C, 3E, 3F, and 3H).

Knockdown of Rpt4 and Rpt5, subunits of the p27 module, caused accumulation of a complex containing Rpt1, Rpt2, Rpn1, Rpt3, and Rpt6, again subunits of the other two modules (Figures 3B–3D, 3G, and 3H). In these knockdowns, Rpn2 appeared as two bands of fast-migrating species; the slower one was likely associated with Rpn13 (Figures 3I and S2). These results suggest that each module behaves as a group during base formation and that preceding association of the three modules is required for efficient incorporation of Rpn2 during the base assembly. However, a portion of the complex that accumulated in Rpt4- and Rpt5-knockdown cells appeared to include Rpn2, suggesting that Rpn2 could be incorporated to some extent in the absence of Rpt4 and Rpt5 (Figure 3I).

Loss of Rpn2 caused accumulation of a complex that included all the ATPase subunits and Rpn1, indicating that Rpn2 is not

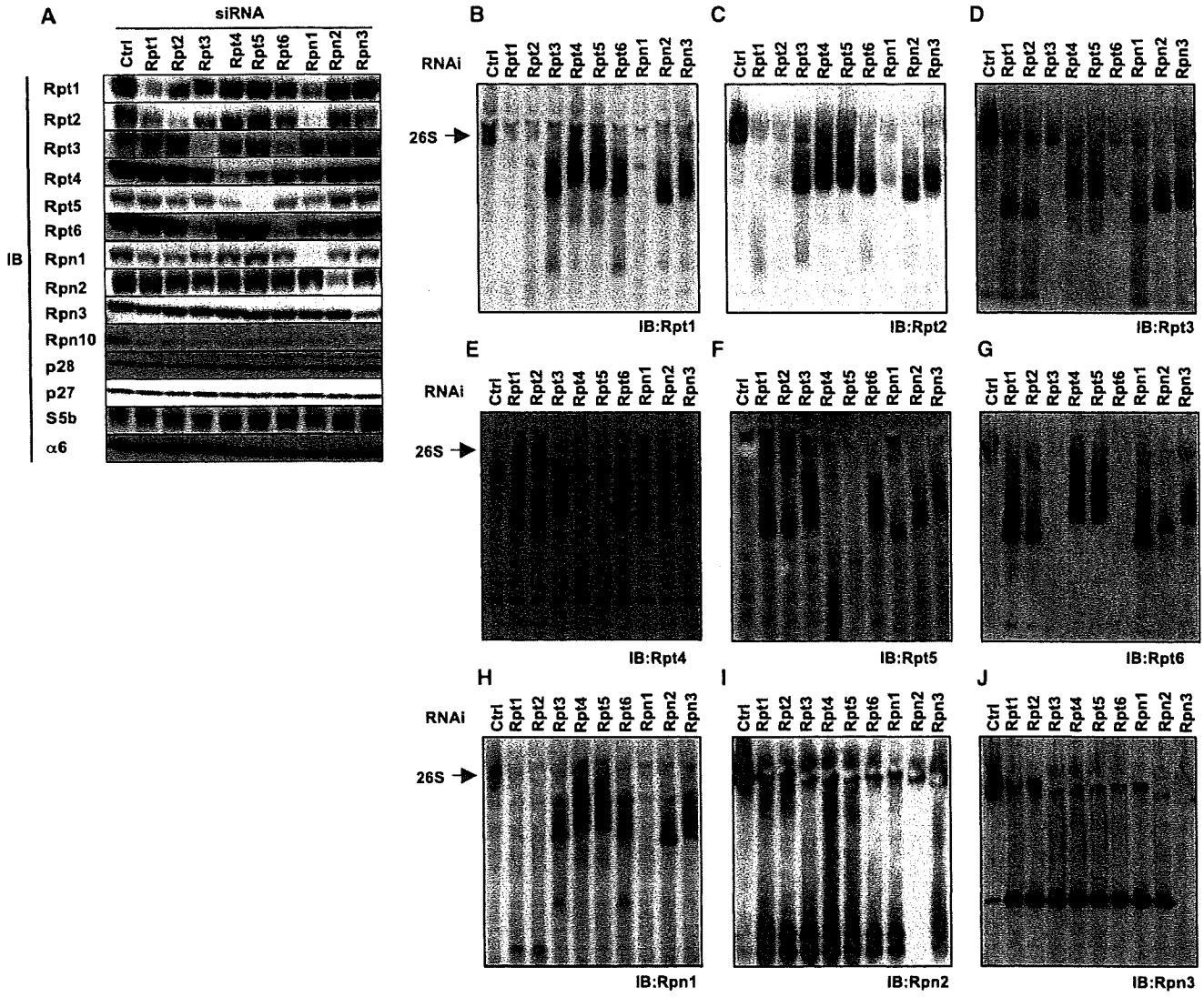

Figure 3. Effects of Knockdown of Base Subunits on the Proteasome Assembly

(A) Whole-cell extracts from HEK293T cells treated with siRNA against base subunits as well as Rpn3 for 48 hr were analyzed by immunoblotting for the expression levels of the indicated proteasome subunits.

(B–J) Cell extracts used in (A) were separated by native-PAGE. Accumulated complexes were detected by immunoblotting with the indicated antibodies. Bands corresponding to the 26S proteasome are depicted by arrows.

a prerequisite for assembly involving the three modules (Figures 3B–3H), although it is also possible that Rpn2 affects the efficiency of the association among the three modules. Knockdown of Rpn3 caused accumulation of the base subcomplex as revealed by detection of all the base subunits, although the presence of Rpn2 was obscure in the native-PAGE analysis (Figure 3I).

On the other hand, the amount of free lid subcomplex that was not associated with the base subcomplex, which was already visible in control cells, increased after knockdown of the base subunits, suggesting that the lid subcomplex efficiently binds to the complete base, further supporting the previous observation that the formation of the base and lid occurs independently (Isono et al., 2007) (Figure 3J).

Hierarchical Assembly of the Modules

Although native-PAGE analysis provides qualitative information about the nature of the accumulated complex, it does not provide reliable quantitative data. For example, the 26S proteasome (observed in control cells) and the base subcomplex (observed in Rpn3-knockdown cells) should include the base subunits with similar stoichiometry, whereas some antibodies (anti-Rpt1, -Rpt4, -Rpt5, and -Rpt6) detected the base complex more strongly than the 26S proteasome and other antibodies exhibited more intense reactivity to the 26S proteasome compared to the base subcomplex. Furthermore, it was difficult to detect the three modules, which were otherwise readily detected in immunoblot analysis after SDS-PAGE of the samples fractionated by glycerol gradient centrifugation (Figure 1A). This may be due to the

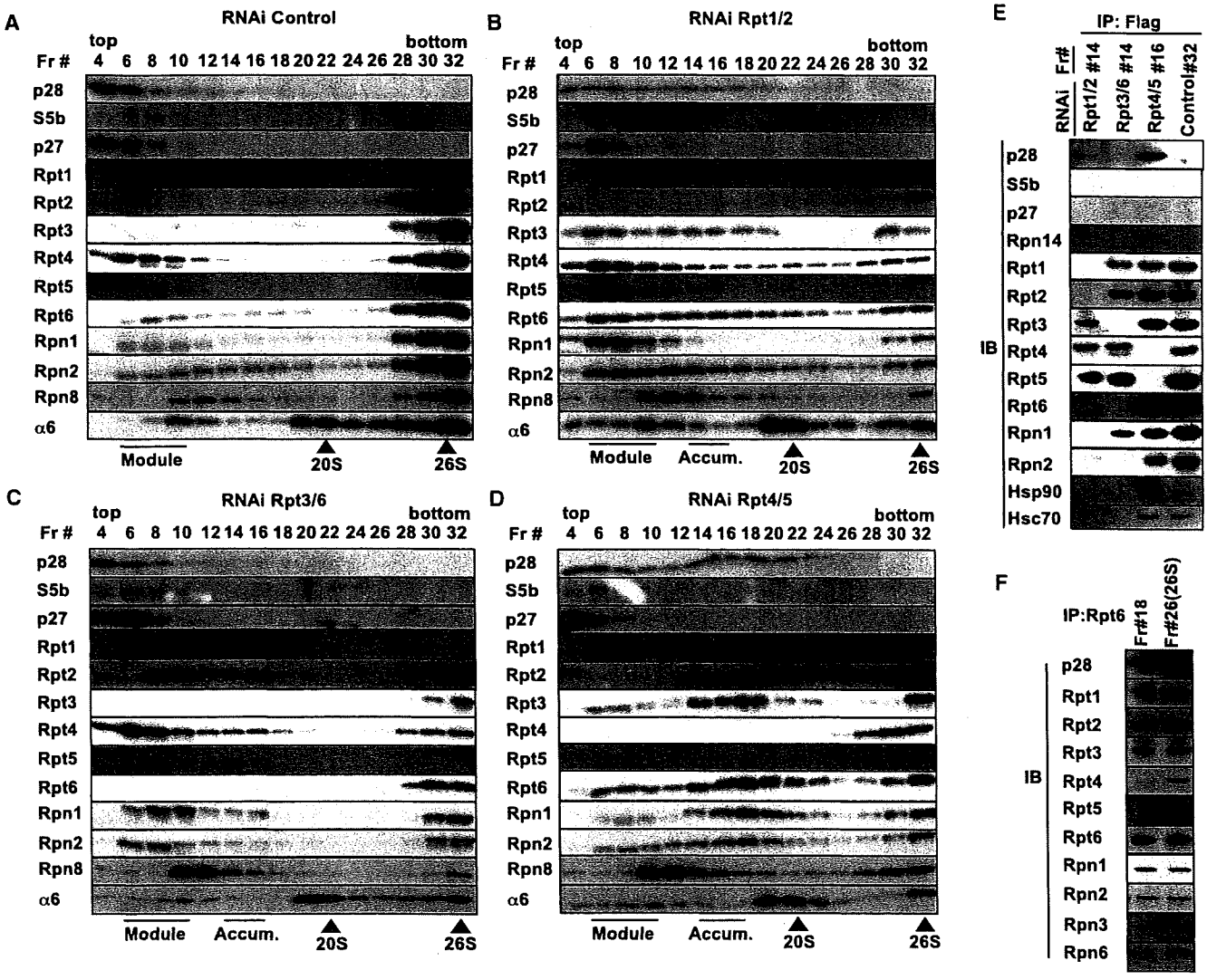

Figure 4. Glycerol Gradient Analysis of Knockdown Cells reveals the Order of Assembly

(A–D) siRNA targeting Rpt1/Rpt2 (B), Rpt3/Rpt6 (C), Rpt4/Rpt5 (D), or control siRNA (A) was transfected into HEK293T cells, and 48 hr after transfection the cells were lysed and subjected to 4%–24% glycerol gradient analysis. The resultant fractions were analyzed by immunoblotting with the indicated antibodies. The positions of the modules, accumulated complexes (Accum.), the CP (20S), and the 26S proteasome are indicated at the bottom of each panel.

(E) HEK293T cells stably expressing Flag-Rpt4 or Flag-Rpt6 were treated with siRNAs targeting Rpt1/2 (in Flag-Rpt4 cells), Rpt3/6 (in Flag-Rpt4 cells), and Rpt4/5 (in Flag-Rpt6 cells), lysed, and subjected to 4%–24% glycerol gradient analysis. The fractions with the accumulated complexes were immunoprecipitated with M2 agarose, followed by immunoblotting with the indicated antibodies. The 26S proteasome was immunoprecipitated from the 26S fraction (Fr#32) of the Flag-Rpt6 cells.

(F) Fractions 18 and 26 (26S fraction) in Figure 1A were immunoprecipitated with anti-Rpt6 antibody. Approximately equimolar amounts of proteasome subunits except Rpt4 and Rpt5 were loaded and analyzed by SDS-PAGE, followed by immunoblotting with the indicated antibodies.

dependence of antibody reactivity on accessibility to the target subunit within the native complex, which makes it difficult to assess quantitative aspects of the complexes.

To overcome this weakness, we fractionated the knockdown cell lysates by glycerol gradient centrifugation, followed by SDS-PAGE and immunoblotting of each fraction. In these experiments, the pairing Rpt subunits were simultaneously knocked down to ensure that the targeted module is completely abrogated (Figures 4A–4D).

In Rpt1/2 knockdown cells, although the accumulated complex observed in native-PAGE analysis was found around fractions 12–16 (Figure 4B), which was a complex between the p28 and p27 modules as revealed by immunoprecipitation analysis (Figure 4E), the most notable change compared to control cells was accumulation of Rpt3, Rpt4, Rpt5, and Rpt6, which are subunits of the p28 module and the p27 module, in the light fractions (fractions 6–8). This finding suggests that the association between the p28 and p27 modules is not efficient in the absence of the S5b module. Rpn1 also accumulated in these light fractions, presumably as a free subunit (Figure 4B), in agreement with the previous finding that Rpn1 was relatively retained even in the absence of Rpt1 and Rpt2 (Figure 3A).

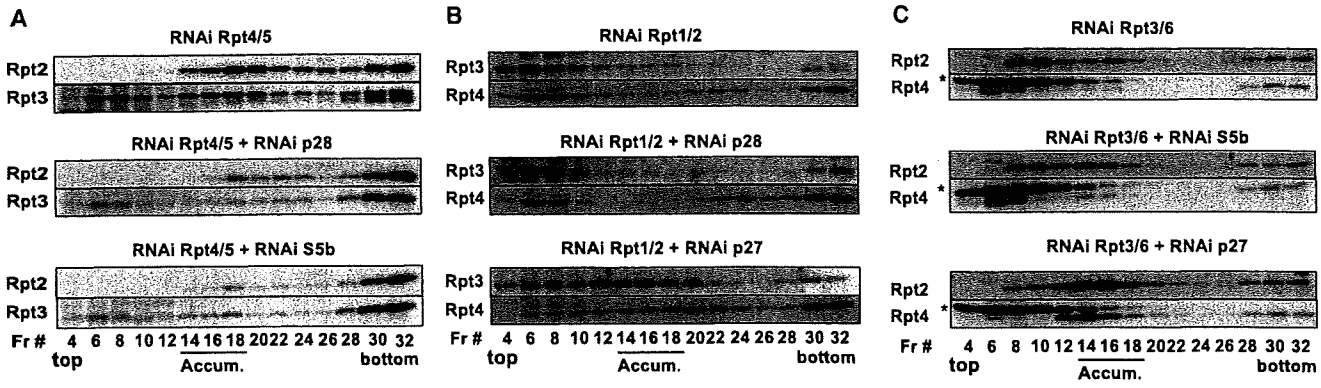

Figure 5. Regulation of Interaction between Various Modules by Base Chaperones

The indicated combinations of siRNAs were transfected into HEK293T cells, where knockdown of p28, S5b, and p27 preceded those of Rpts by 48 hr. Forty-eight hours after transfection of siRNAs against Rpt subunits, cells were lysed and subjected to 4%–24% glycerol gradient centrifugation. Fractions were immunoblotted as indicated. The positions of the accumulated complexes are indicated (Accum.).

Similarly, in Rpt3/6-knockdown cells, although the accumulated complex resulting from association between the S5b and the p27 modules, as revealed by immunoprecipitation analysis (Figure 4E), was detected around fractions 14–16, they exhibited obvious accumulation of free S5b and p27 modules, suggesting that the association between the S5b and p27 modules is inefficient without the p28 module (Figure 4C).

In contrast to Rpt1/2- and Rpt3/6-knockdown cells, Rpt4/5-knockdown cells showed much less accumulation of free p28 and S5b modules. Instead, they showed accumulation of a complex formed by the assembly of the p28 and the S5b modules around fractions 14–20, which was confirmed by immunoprecipitation analysis (Figures 4D and 4E). Rpn2 was substantially incorporated in this complex (Figures 4D and 4E), supporting the notion that Rpn2 could be incorporated before incorporation of Rpt4 and Rpt5, as suggested in Figure 3I. However, this is inconsistent with native-PAGE analysis in that increase in free Rpn2 was not obvious in glycerol gradient analysis, which may be due to differences in the experimental procedure. p28 and Rpn14 were also included in this complex, but not S5b, indicating that S5b, if not all, dissociate upon binding to the p28 module while p28 and Rpn14 continue to be associated throughout the base formation (Figures 4D and 4E). p28 was also retained upon association of the p28 module with the p27 module observed in Rpt1/2-knockdown cells (Figures 4B and 4E). Both S5b and p27 were hardly observed in any of the complexes formed by either two of the modules (Figures 4B–4E). Despite the lack of two or three base subunits, the accumulated complexes in Rpt-knockdown cells were comparable in size with or even larger than the purified base subcomplex in case of Rpt4/5 knockdown cells (see Figure S3 for the position of the purified base in the similar glycerol gradient analysis; also compare complexes accumulated in Rpn3 RNAi with those in Rpts RNAi in native-PAGE analyses shown in Figure 3). Interestingly, general chaperones such as Hsp90 and Hsc70 were associated with the complex accumulated in Rpt4/5 knockdown cells, possibly because of the unstable nature of this complex (Figure 4E), which may at least in part account for unexpectedly large size of the complex. It is also possible that they were associated with some unidentified molecules, constituted in abnormal stoichiometries, or prone to form aggregates.

These results suggest that the base formation starts with an association between the p28 module and the S5b module and that the p27 module is the last module incorporated during the base assembly.

19S RP-like Complex Lacking Rpt4 and Rpt5 in Mammalian Cells

We noticed that fractions 18–20 in Figure 1A, which correspond to the size of the CP as revealed by immunoblot for the α6 subunit, seemed to contain both the base and lid subunits, except for Rpt4 and Rpt5 (Figure 1A). To verify the composition of this complex, we immunoprecipitated fraction 18 and fraction 26 (26S proteasome fraction) in Figure 1A with anti-Rpt6 antibody, and then immunoblotted for all the base subunits as well as some of the lid subunits. While the 26S proteasome contained all the subunits examined, the precipitated complex of fraction 18 included other base subunits as well as lid subunits but was specifically deficient in Rpt4 and Rpt5 (Figure 4F). This is the first identification of the presence of 19S RP-like complex lacking two of the ATPase subunits in mammalian cells.

Importantly, p28 was found abundantly in this RP-like complex (Figure 4F), suggesting that it possibly represents a complex before incorporation of the p27 module on the maturation pathway of the RP. These findings further support the model in which the p27 module is the last to incorporate during the base formation and suggests that the lid can associate with the base without Rpt4 and Rpt5.

Roles of p28, S5b, and p27 during Base Assembly

As shown in Figure 4, the association of the p28 module with the S5b module is likely the initial step of the base formation. To clarify the role of p28 and S5b in this association, we knocked down either of the two concurrently with Rpt4 and Rpt5. Notably, the complex that accumulated in Rpt4/5-knockdown cells around fraction 18 was markedly deficient either by p28 or S5b knockdown (Figure 5A). Loss of the accumulated complex was reproduced in native-PAGE analysis of Rpt4/5/p28-knockdown

cells, but the effect of S5b knockdown was not as apparent as in glycerol gradient analysis (Figure S4A). These results suggest that p28, and possibly S5b, facilitates or stabilizes the association between the p28 module and S5b module, although free forms of Rpt2 and Rpt3 or aggregated forms of the accumulated complex, which would be expected to increase, were not observed (Figure 5A).

We also tested whether p28, S5b, and p27 affect the association among other combinations of the modules. Intriguingly, concurrent loss of p27 with Rpt1/2 and Rpt3/6 knockdowns augmented the association of the Rpt4/Rpt5 with the p28 module and S5b module, respectively, as confirmed by immunoprecipitation analysis (Figures 5B and 5C, bottom panels, and Figure S4B). These results suggest that p27 plays an inhibitory role in these combinations of association, which are not supposed to occur in normal cells as suggested in Figure 4. Increase in the accumulated complex upon p27 knockdown was also observed in native-PAGE analysis, further confirming the inhibitory role of p27 (Figures S4C and S4D). Loss of p28 in the Rpt1/2-knockdown cells decreased the accumulated complex found around fraction 16 (Figure 5B, middle, and Figure S2C), suggesting that p28 was also involved in the association between the p28 module and p27 module. On the other hand, S5b did not appear to have enhancing or inhibitory effects on the association of the p27 module with the S5b module (Figure 5C, middle, and Figure S4D).

In the sense that p28, S5b, and p27 associate with "immature" forms of subunits that are destined to formation of functional proteasomes, where these three molecules regulate associations between subunits, it is reasonable to refer to them as proteasome assembly chaperones.

Loss of Chaperones Causes Mild but Significant Defects in 19S RP Assembly

To clarify the importance of these chaperones in proteasome function and assembly, we knocked each of them down alone, not in combination with base subunits. Knockdown of p28, S5b, or p27 reduced the peptidase activity of the 26S proteasome by approximately 20%–35% compared to the control RNAi (Figure 6A) and caused accumulation of ubiquitinated proteins (Figure 6B, bottom), confirming that these chaperones are truly involved in the integrity of the 26S proteasome. However, the cells continued to grow at a rate comparable with control cells, at least during 6 day knockdown (data not shown), suggesting that mammalian cells can produce 26S proteasomes sufficient to survive without these chaperones at least under normal conditions.

To determine whether loss of these chaperones affects the stability of the base subunits, we examined the expression levels of proteasome subunits in these cells. While knockdown of p28 and S5b did not significantly affect the expression of base subunits, including their partner subunits within the modules, loss of p27 caused reduction in Rpt4 and Rpt5 (Figure 6B). Subsequent analysis revealed that p27 is necessary for stable expression of a free form of the p27 module (Figure 6E) and not for all the Rpt4 and Rpt5 expressions since continuous knockdown of p27 did not cause cell death while Rpt4 and Rpt5 are essential for cell growth (data not shown).

We also explored the type of assembly defect in these knockdown cells by subjecting the cell lysates to glycerol gradient analysis (Figures 6C–6E). Knockdown of p28 caused accumulation of Rpt3, Rpt6 and the S5b and p27 modules in light fractions (Figure 6D, fractions 6–12). This is consistent with the notion that p28 promotes the initial step of the base assembly, i.e., the association between the p28 module and S5b module. In addition, p28-knockdown cells showed accumulation of a complex of a size between the 20S and 26S around fraction 22, which seemed to contain only base subunits. To confirm the composition of this complex, we immunoprecipitated fraction 22 with anti-Rpt6 antibody and compared its contents with those of the 26S proteasome. As expected, this complex contained a full set of the base subunits but not lid subunits nor the CP subunits (Figure 6F). Since it was larger than the purified base (Figure S3), it is likely aggregates of the base subcomplex. This suggests that p28 has another role in preventing aggregation of the assembled base subcomplex. In contrast, we could not find evidence for assembly defect in S5b-knockdown cells (Figure S5), which were expected to show similar phenotypes as p28 knockdown, considering the result shown in Figure 5A. As suggested by the low degree of reduction in proteasome activity compared to p28 knkockdown (Figure 6A), the contribution of S5b might be so small that we could not detect specific defects in the base assembly.

p27 knockdown caused loss of Rpt4 and Rpt5 in the light fractions, which was readily observed in control cells (Figure 6E), thus accounting for the reduced Rpt4 and Rpt5 levels in whole-cell lysates (Figure 6B). p27-knockdown cells exhibited phenotypes similar to those of Rpt4/5-knockdown cells (Figure 4D). They showed no accumulation of the p28 module or the S5b module and instead showed accumulation of the complex comprising the p28 and S5b modules and lacking Rpt4 and Rpt5 (Figure 6E, fraction 18), which was further confirmed by comparison of its composition with the 26S proteasome (Figure 6G).

Rpn14 knockdown did not alter the activity of the 26S proteasome or the distribution of the base subunits (Figure S6), suggesting that Rpn14 does not play an important role in the RP assembly, at least in mammalian cells.

We next examined the effect of simultaneous knockdown of the assembly chaperones. However, no additive effect was obtained, with p28 single knockdown showing the highest reduction in the 26S activity (Figure S7), consistent with the notion that p28 catalyzes an initial step of the base assembly.

Finally, we examined protein stabilities of p28, S5b, p27, and Rpn14 by a cycloheximide-chase assay. These were rather stable proteins, compared to hUmp1, which is a CP assembly chaperone know to be degraded concurrently with CP formation (Figure S8). This suggests that the base assembly chaperones dissociate during the RP formation and are recycled.

DISCUSSION

Our results allow us to design a model for the assembly pathway of the base subcomplex of the mammalian proteasome (Figure 7). Individual base subunits, with the exception of Rpn2, cannot stand alone and need to be paired with a particular subunit(s) (Figure 3A). The paired subunits are associated with

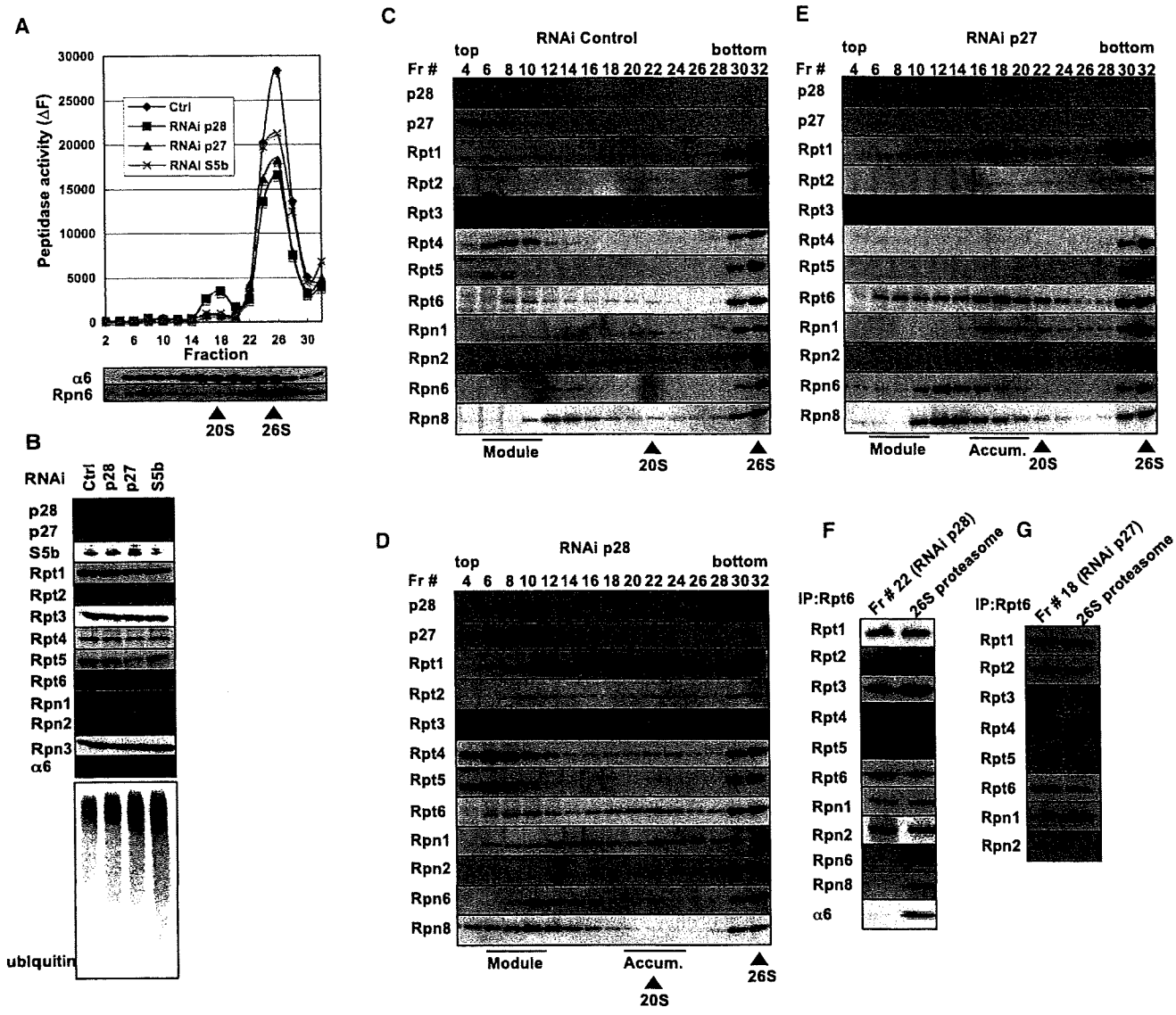

Figure 6. Knockdown of Base Chaperones Causes Defective Assembly of the RP

(A) Cell extracts from HEK293T cells treated with siRNAs against p28, p27, and S5b for 72 hr were fractionated by 8%–32% glycerol gradient centrifugation and assayed for Suc-LLVY-MCA hydrolyzing activity. Immunoblots for a CP subunit (α6) and an RP subunit (Rpn6) were shown to indicate the position of the 26S proteaosme.

(B) Immunoblot analysis of whole-cell extracts used in (A).

(C–E) siRNA targeting p28 (D), p27 (E), or control siRNA (C) was transfected into HEK293T cells, and the cell lysates were fractionated by 4%–24% glycerol gradient centrifugation. The resultant fractions were analyzed by immunoblotting with the indicated antibodies. The positions of the modules, accumulated complexes (Accum.), the CP (20S), and the 26S proteasome are indicated at the bottom of each panel.

(F) Fractions 22 and 32 (26S) in (D) were immunoprecipitated with anti-Rpt6 antibody. The resultant samples were loaded so that approximately equimolar amounts of Rpt subunits were included and analyzed by SDS-PAGE, followed by immunoblotting with the indicated antibodies.

(G) Fractions 18 and 32 (26S) in (E) were immunoprecipitated with anti-Rpt6 antibody and analyzed as in (F).

proteasome-dedicated chaperones that directly interact with specific ATPase subunits, thus shaping three distinct modules (Figures 1 and 2). These three modules serve as parts for the base assembly (Figures 3B–3H), where the chaperones are involved in the association between the modules (Figures 5 and S4). While p28, and possibly S5b, positively regulates the association between the Rpt3-Rpt6 complex and the Rpt1-Rpt2-Rpn1 complex, p27 inhibits the association of the Rpt4-Rpt5 complex with the other two complexes (Figures 5 and S4). Consequently, the assembly of the base subcomplex begins with the association between the p28 module and S5b module (Figure 4).

While p28 and S5b are not required for the stability of the associating subunits, p27 plays a key role in the expression of a free

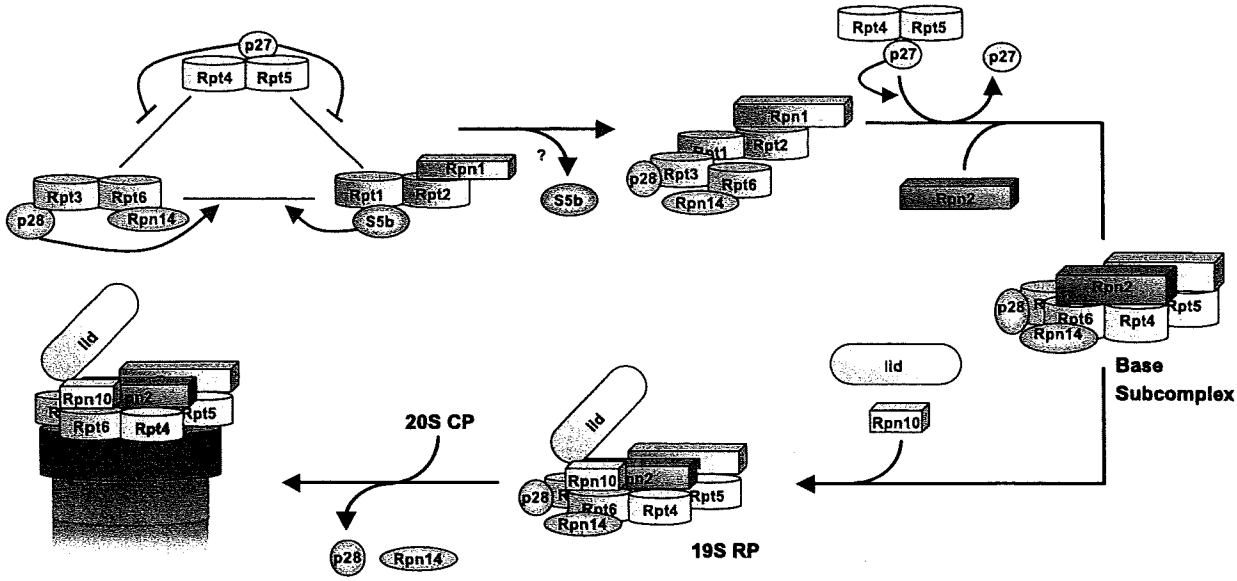

Figure 7. A schematic Model of the 19S RP Assembly and Roles of Base-Specific Chaperones

Base subunits, with the exception of Rpn2, form a complex in specific combinations, where proteasome-dedicated chaperones directly interact with specific ATPase subunits, thus shaping three distinct modules. While p28 and S5b positively regulate the association between the Rpt3-Rpt6 complex and the Rpt1-Rpt2-Rpn1 complex, p27 inhibits the association of the Rpt4-Rpt5 complex with the other two complexes. Accordingly, the assembly of the base subcomplex begins with the association between the p28 module and S5b module, followed by incorporation of the p27 module and Rpn2. See the Discussion for details.

form of the p27-Rpt5-Rpt4 complex (Figures 6B and 6E). The complex formation of Rpt4-Rpt5 with p27 is important for orderly assembly of the base subcomplex. Loss of p27 causes uncontrolled incorporation of Rpt4-Rpt5, resulting in premature association of Rpt4-Rpt5 with the p28 and S5b modules (Figures 5B, 5C, S4C, and S4D). After the legitimate complex formation between the p28 module and S5b module, p27, in turn, promotes the incorporation of Rpt4-Rpt5 into the complex (Figure 6E). The association between the p28 module and S5b module seems to be more efficient than the association of uncontrolled Rpt4-Rpt5 with the p28 module or the S5b module since p27-knockdown cells did not accumulate a complex containing Rpt4 and Rpt5 (Figure 6E).

It is still ambiguous which is incorporated earlier to the complex made of p28 and S5b modules, Rpn2 or the p27 module. It is reasonable that the p27 module precedes Rpn2 since lack of Rpt4 and Rpt5 was associated with accumulation of free Rpn2 in native-PAGE analysis (Figure 3I), but there seems to be at least some fractions of the assembly process where incorporation of the p27 module is the final step of the RP assembly, as suggested by the presence of 19S RP-like complex lacking Rpt4 and Rpt5 in intact cells (Figure 4E).

p28 is likely associated with the base throughout the assembly of the RP, as suggested by the data displayed in Table S1 and Figure 4E. With regard to S5b, mass spectrometric analysis suggests that it is also associated with the base subunit until completion of the 19S RP assembly, but we could not verify this by biochemical analysis (Figures 4C–4E). This may be simply due to the sensitivity of antibody detection. p27 is likely to be detached upon incorporation of the p27 module, which is indicated by both mass spectrometry and biochemical experiments (Table S1 and Figures 4B–4E). The complete base (or semicomplete base lacking Rpt4 and Rpt5) is assembled with Rpn10 and the lid subcomplex, which is formed independently of the base subcomplex, thus building the RP (Figure 7).

Despite the elaborate mechanism, p28, S5b, and p27, as well as Rpn14, are not prerequisite for cell viability, at least in our experiment. This suggests that a large portion of the proteasome can be correctly assembled in the absence of these chaperones and that they are probably required under certain unconventional situations where more efficient proteasome assembly is needed. In this sense, it is intriguing that one of these chaperones, p28, is designated as an oncogene. p28 was rediscovered during a search for genes overexpressed in hepatocellular carcinoma (HCC), independently of the relevance to the proteasome, and therefore it was referred to as "gankyrin" (gann stands for cancer in Japanese) (Higashitsuji et al., 2000). PAC2, a proteasome assembly chaperone for the CP formation, was also initially identified as a gene overexpressed in HCC (Wang et al., 2001), and PAC1, another CP assembly chaperone, has been reported to be upregulated in growing cells (Vidal-Taboada et al., 2000). These results suggest that such proteasome assembly chaperones are needed for production of sufficient proteasomes in rapidly proliferating cells such as malignant cells, although whether the oncogenicity of p28/gankyrin is related to the proteasome assembly is not clear at present.

Our data may also explain at least part of the curious "modulator" effect exerted by the p27-Rpt5-Rpt4 complex (Adams et al., 1997; DeMartino et al., 1996). We demonstrated that there is a pool of the RP-like complex that is deficient specifically in Rpt4 and Rpt5 (Figure 4F). Since Rpt5 is a key subunit in binding of the RP to the α ring of the CP via its C-terminal motif (Gillette

et al., 2008; Smith et al., 2007), the addition of the p27-Rpt5-Rpt4 complex to the purified RP, which probably contains such RP-like complex, makes up complete RP that can fully associate with and activate the CP. We were able to recapitulate the modulator effect by mixing the fractions corresponding to the RP-like complex and the p27 module together with purified CPs (data not shown), although it was difficult to verify that the p27-Rpt5-Rpt4 complex exogenously added to the RP-like complex in vitro is indeed incorporated in the correct positions of the ATPase hexameric ring.

During the preparation of this manuscript, Le Tallec et al. reported Hsm3, a yeast homolog of mammalian S5b, as a chaperone for the base assembly (Le Tallec et al., 2009). Hsm3 forms a complex with Rpt1, Rpt2, and Rpn1 in yeast, which is identical to our result in mammalian cells. Hsm3 is required for the association of Rpt1 with Rpt2 and Rpn1, but the same role does not seem to be applied to S5b in mammalian cells since loss of S5b did not affect the expression level of Rpt2 (Figure 6B), which should be reduced in the absence of Rpt1 if S5b were required for association of Rpt2 with Rpt1. Moreover, although Rpn14 is a component of the p28 module, knockdown of human Rpn14 in HEK293T cells did not show any obvious effect (Figure S5); rather, it was reported to enhance the proteasome activity in HeLa cells (Park et al., 2005). In contrast, yeast Rpn14 is apparently involved in the base assembly (Saeki et al., 2009). Therefore, the role of Rpn14 also appears to be different between yeast and mammals.

In sum, our present study provides evidence that base specific chaperones coordinate the association among the base subunits, hence facilitating the assembly of the base subcomplex. Further studies are needed to clarify the mechanisms involved in the recognition and regulation of subunit interactions by the individual chaperones.

EXPERIMENTAL PROCEDURES

DNA Constructs

The cDNAs encoding p28, S5b, and p27 were isolated from HEK293T cells by RT-PCR using total RNA and were subcloned into pIRESpuro3 (Clontech). All constructs were confirmed by sequencing.

Protein Extraction and Biochemical Analysis

Cells were lysed in an ice-cold lysis buffer (50 mM Tris-HCl [pH 7.5], 0.5% [v/v] NP-40, 1 mM dithiothreitol, 2 mM ATP, and 5 mM $MgCl_2$), and the extracts were clarified by centrifugation at 20,000 × g for 15 min at 4°C. The supernatants were subjected to glycerol gradient or native-PAGE analysis. The methods used for glycerol gradient centrifugation and assay of proteasome activity with succinyl-Leu-Leu-Val-Tyr-7-amido-4-methylcoumarin (Suc-LLVY-MCA) were described previously (Murata et al., 2001). In vitro transcription and translation followed by binding assay was described previously (Hirano et al., 2005). Native-PAGE (3%–8% Tris-Acetate gel [Invitrogen]) was performed according to the instructions provided by the manufacturer.

Immunological Analysis and Antibodies

The separated proteins were transferred onto polyvinylidene difluoride membrane and subjected to immunoblot analysis. For immunoprecipitation, we used anti-Rpt6 monoclonal antibody crosslinked to NHS-activated Sepharose (GE) or M2 agarose (Sigma). These beads were added to the extracts, mixed under constant rotation for 2 hr at 4°C, washed with lysis buffer, and boiled in SDS sample buffer. Otherwise, the washed samples were eluted with 100 μg/ml Flag peptides (Sigma) or with 0.2 M glycine-HCl (pH 2.8). Polyclonal antibodies against human p28, p27, S5b, Rpn14, Rpn6, and Rpn8 were raised in rabbits with the following recombinant proteins expressed in and purified from BL21RIL strain (Novagen) as His-tag fusion proteins: p28 (full length), p27 (full length), S5b (full length), Rpn14 (residues 209–392), Rpn6 (residues 172–422), and Rpn8 (full length). Antibodies against hUmp1, Rpt1–6, Rpn1–3, Rpn10, and Rpn13 were described previously (Hamazaki et al., 2006; Hirano et al., 2005; Tanahashi et al., 2000). The antibodies for polyubiquitin, Hsp90, and Hsc70 were purchased (MBL).

RNA Interference

The siRNAs were from Invitrogen (sequences are shown in Table S2). They were transfected into HEK293T cells with Lipofectamine RNAi MAX (Invitrogen) at a final concentration of 50 nM in 10 cm dishes.

SUPPLEMENTAL DATA

Supplemental Data include Supplemental Experimental Procedures, eight figures, and two tables and can be found with this article online at http://www.cell.com/supplemental/S0092-8674(09)00565-0.

ACKNOWLEDGMENTS

This work was supported by grants from the Ministry of Education, Science, and Culture of Japan (MEXT; to S.M. and K.T.), the Takeda Science Foundation (to S.M. and K.T.), Target Protein Project of MEXT (to K.T.), and the New Energy and Industrial Technology Development Organization (to T.N.).

Received: March 23, 2009
Revised: May 1, 2009
Accepted: May 8, 2009
Published: May 28, 2009

REFERENCES

Adams, G.M., Falke, S., Goldberg, A.L., Slaughter, C.A., DeMartino, G.N., and Gogol, E.P. (1997). Structural and functional effects of PA700 and modulator protein on proteasomes. J. Mol. Biol. *273*, 646–657.

Baumeister, W., Walz, J., Zuhl, F., and Seemuller, E. (1998). The proteasome: paradigm of a self-compartmentalizing protease. Cell *92*, 367–380.

Coux, O., Tanaka, K., and Goldberg, A.L. (1996). Structure and functions of the 20S and 26S proteasomes. Annu. Rev. Biochem. *65*, 801–847.

Dawson, S., Apcher, S., Mee, M., Higashitsuji, H., Baker, R., Uhle, S., Dubiel, W., Fujita, J., and Mayer, R.J. (2002). Gankyrin is an ankyrin-repeat oncoprotein that interacts with CDK4 kinase and the S6 ATPase of the 26 S proteasome. J. Biol. Chem. *277*, 10893–10902.

Dawson, S., Higashitsuji, H., Wilkinson, A.J., Fujita, J., and Mayer, R.J. (2006). Gankyrin: a new oncoprotein and regulator of pRb and p53. Trends Cell Biol. *16*, 229–233.

DeMartino, G.N., Proske, R.J., Moomaw, C.R., Strong, A.A., Song, X., Hisamatsu, H., Tanaka, K., and Slaughter, C.A. (1996). Identification, purification, and characterization of a PA700-dependent activator of the proteasome. J. Biol. Chem. *271*, 3112–3118.

Deveraux, Q., Jensen, C., and Rechsteiner, M. (1995). Molecular cloning and expression of a 26 S protease subunit enriched in dileucine repeats. J. Biol. Chem. *270*, 23726–23729.

Gillette, T.G., Kumar, B., Thompson, D., Slaughter, C.A., and Demartino, G.N. (2008). Differential roles of the C-termini of AAA subunits of PA700 (19S regulator) in asymmetric assembly and activation of the 26s proteasome. J. Biol. Chem. *283*, 31813–31822.

Glickman, M.H., Rubin, D.M., Coux, O., Wefes, I., Pfeifer, G., Cjeka, Z., Baumeister, W., Fried, V.A., and Finley, D. (1998). A subcomplex of the proteasome regulatory particle required for ubiquitin-conjugate degradation and related to the COP9-signalosome and eIF3. Cell *94*, 615–623.

Gomes, A.V., Zong, C., Edmondson, R.D., Li, X., Stefani, E., Zhang, J., Jones, R.C., Thyparambil, S., Wang, G.W., Qiao, X., et al. (2006). Mapping the murine cardiac 26S proteasome complexes. Circ. Res. *99*, 362–371.

Hamazaki, J., Iemura, S., Natsume, T., Yashiroda, H., Tanaka, K., and Murata, S. (2006). A novel proteasome interacting protein recruits the deubiquitinating enzyme UCH37 to 26S proteasomes. EMBO J. *25*, 4524–4536.

Hershko, A., and Ciechanover, A. (1998). The ubiquitin system. Annu. Rev. Biochem. *67*, 425–479.

Higashitsuji, H., Itoh, K., Nagao, T., Dawson, S., Nonoguchi, K., Kido, T., Mayer, R.J., Arii, S., and Fujita, J. (2000). Reduced stability of retinoblastoma protein by gankyrin, an oncogenic ankyrin-repeat protein overexpressed in hepatomas. Nat. Med. *6*, 96–99.

Hirano, Y., Hendil, K.B., Yashiroda, H., Iemura, S., Nagane, R., Hioki, Y., Natsume, T., Tanaka, K., and Murata, S. (2005). A heterodimeric complex that promotes the assembly of mammalian 20S proteasomes. Nature *437*, 1381–1385.

Hori, T., Kato, S., Saeki, M., DeMartino, G.N., Slaughter, C.A., Takeuchi, J., Toh-e, A., and Tanaka, K. (1998). cDNA cloning and functional analysis of p28 (Nas6p) and p40.5 (Nas7p), two novel regulatory subunits of the 26S proteasome. Gene *216*, 113–122.

Isono, E., Nishihara, K., Saeki, Y., Yashiroda, H., Kamata, N., Ge, L., Ueda, T., Kikuchi, Y., Tanaka, K., Nakano, A., et al. (2007). The assembly pathway of the 19S regulatory particle of the yeast 26S proteasome. Mol. Biol. Cell *18*, 569–580.

Jorgensen, J.P., Lauridsen, A.M., Kristensen, P., Dissing, K., Johnsen, A.H., Hendil, K.B., and Hartmann-Petersen, R. (2006). Adrm1, a putative cell adhesion regulating protein, is a novel proteasome-associated factor. J. Mol. Biol. *360*, 1043–1052.

Kusmierczyk, A.R., and Hochstrasser, M. (2008). Some assembly required: dedicated chaperones in eukaryotic proteasome biogenesis. Biol. Chem. *389*, 1143–1151.

Le Tallec, B., Barrault, M.B., Guerois, R., Carre, T., and Peyroche, A. (2009). Hsm3/S5b participates in the assembly pathway of the 19S regulatory particle of the proteasome. Mol. Cell *33*, 389–399.

Meiners, S., Heyken, D., Weller, A., Ludwig, A., Stangl, K., Kloetzel, P.M., and Kruger, E. (2003). Inhibition of proteasome activity induces concerted expression of proteasome genes and de novo formation of Mammalian proteasomes. J. Biol. Chem. *278*, 21517–21525.

Murata, S., Udono, H., Tanahashi, N., Hamada, N., Watanabe, K., Adachi, K., Yamano, T., Yui, K., Kobayashi, N., Kasahara, M., et al. (2001). Immunoproteasome assembly and antigen presentation in mice lacking both PA28alpha and PA28beta. EMBO J. *20*, 5898–5907.

Murata, S., Yashiroda, H., and Tanaka, K. (2009). Molecular mechanisms of proteasome assembly. Nat. Rev. Mol. Cell Biol. *10*, 104–115.

Nakamura, Y., Nakano, K., Umehara, T., Kimura, M., Hayashizaki, Y., Tanaka, A., Horikoshi, M., Padmanabhan, B., and Yokoyama, S. (2007). Structure of the oncoprotein gankyrin in complex with S6 ATPase of the 26S proteasome. Structure *15*, 179–189.

Natsume, T., Yamauchi, Y., Nakayama, H., Shinkawa, T., Yanagida, M., Takahashi, N., and Isobe, T. (2002). A direct nanoflow liquid chromatography-tandem mass spectrometry system for interaction proteomics. Anal. Chem. *74*, 4725–4733.

Park, Y., Hwang, Y.P., Lee, J.S., Seo, S.H., Yoon, S.K., and Yoon, J.B. (2005). Proteasomal ATPase-associated factor 1 negatively regulates proteasome activity by interacting with proteasomal ATPases. Mol. Cell. Biol. *25*, 3842–3853.

Qiu, X.B., Ouyang, S.Y., Li, C.J., Miao, S., Wang, L., and Goldberg, A.L. (2006). hRpn13/ADRM1/GP110 is a novel proteasome subunit that binds the deubiquitinating enzyme, UCH37. EMBO J. *25*, 5742–5753.

Rabl, J., Smith, D.M., Yu, Y., Chang, S.C., Goldberg, A.L., and Cheng, Y. (2008). Mechanism of gate opening in the 20S proteasome by the proteasomal ATPases. Mol. Cell *30*, 360–368.

Ramos, P.C., and Dohmen, R.J. (2008). PACemakers of proteasome core particle assembly. Structure *16*, 1296–1304.

Ravid, T., and Hochstrasser, M. (2008). Diversity of degradation signals in the ubiquitin-proteasome system. Nat. Rev. Mol. Cell Biol. *9*, 679–690.

Richmond, C., Gorbea, C., and Rechsteiner, M. (1997). Specific interactions between ATPase subunits of the 26 S protease. J. Biol. Chem. *272*, 13403–13411.

Rosenzweig, R., and Glickman, M.H. (2008). Chaperone-driven proteasome assembly. Biochem. Soc. Trans. *36*, 807–812.

Saeki, Y., Toh-e, A., Kudo, T., Kawamura, H., and Tanaka, K. (2009). Multiple proteasome-interacting proteins assist the assembly of the yeast 19S regulatory particle. Cell *137*, this issue, 900–913.

Schwartz, A.L., and Ciechanover, A. (2009). Targeting proteins for destruction by the ubiquitin system: implications for human pathobiology. Annu. Rev. Pharmacol. Toxicol. *49*, 73–96.

Smith, D.M., Chang, S.C., Park, S., Finley, D., Cheng, Y., and Goldberg, A.L. (2007). Docking of the proteasomal ATPases' carboxyl termini in the 20S proteasome's alpha ring opens the gate for substrate entry. Mol. Cell *27*, 731–744.

Tanahashi, N., Murakami, Y., Minami, Y., Shimbara, N., Hendil, K.B., and Tanaka, K. (2000). Hybrid proteasomes. Induction by interferon-gamma and contribution to ATP-dependent proteolysis. J. Biol. Chem. *275*, 14336–14345.

Verma, R., Chen, S., Feldman, R., Schieltz, D., Yates, J., Dohmen, J., and Deshaies, R.J. (2000). Proteasomal proteomics: identification of nucleotide-sensitive proteasome-interacting proteins by mass spectrometric analysis of affinity-purified proteasomes. Mol. Biol. Cell *11*, 3425–3439.

Verma, R., Aravind, L., Oania, R., McDonald, W.H., Yates, J.R., 3rd, Koonin, E.V., and Deshaies, R.J. (2002). Role of Rpn11 metalloprotease in deubiquitination and degradation by the 26S proteasome. Science *298*, 611–615.

Vidal-Taboada, J.M., Lu, A., Pique, M., Pons, G., Gil, J., and Oliva, R. (2000). Down syndrome critical region gene 2: expression during mouse development and in human cell lines indicates a function related to cell proliferation. Biochem. Biophys. Res. Commun. *272*, 156–163.

Wang, X., and Huang, L. (2008). Identifying dynamic interactors of protein complexes by quantitative mass spectrometry. Mol. Cell. Proteomics *7*, 46–57.

Wang, X., Chen, C.F., Baker, P.R., Chen, P.L., Kaiser, P., and Huang, L. (2007). Mass spectrometric characterization of the affinity-purified human 26S proteasome complex. Biochemistry *46*, 3553–3565.

Wang, Z.X., Hu, G.F., Wang, H.Y., and Wu, M.C. (2001). Expression of liver cancer associated gene HCCA3. World J. Gastroenterol. *7*, 821–825.

Watanabe, T.K., Saito, A., Suzuki, M., Fujiwara, T., Takahashi, E., Slaughter, C.A., DeMartino, G.N., Hendil, K.B., Chung, C.H., Tanahashi, N., et al. (1998). cDNA cloning and characterization of a human proteasomal modulator subunit, p27 (PSMD9). Genomics *50*, 241–250.

Yao, T., and Cohen, R.E. (2002). A cryptic protease couples deubiquitination and degradation by the proteasome. Nature *419*, 403–407.

Yao, T., Song, L., Xu, W., DeMartino, G.N., Florens, L., Swanson, S.K., Washburn, M.P., Conaway, R.C., Conaway, J.W., and Cohen, R.E. (2006). Proteasome recruitment and activation of the Uch37 deubiquitinating enzyme by Adrm1. Nat. Cell Biol. *8*, 994–1002.

Immunity

Thymoproteasome Shapes Immunocompetent Repertoire of CD8$^+$ T Cells

Takeshi Nitta,[1] Shigeo Murata,[3] Katsuhiro Sasaki,[4] Hideki Fujii,[5] Adiratna Mat Ripen,[1] Naozumi Ishimaru,[2] Shigeo Koyasu,[5,6] Keiji Tanaka,[4] and Yousuke Takahama[1,*]
[1]Division of Experimental Immunology, Institute for Genome Research
[2]Department of Pathology, Institute for Health Bioscience
University of Tokushima, Tokushima 770-8503, Japan
[3]Laboratory of Protein Metabolism, Graduate School of Pharmaceutical Sciences, University of Tokyo, Tokyo 113-0033, Japan
[4]Laboratory of Frontier Science, Tokyo Metropolitan Institute of Medical Science, Tokyo 156-8506, Japan
[5]Department of Microbiology and Immunology, Keio University School of Medicine, Tokyo 160-8582, Japan
[6]Research Center for Science Systems, Japan Society for the Promotion of Science, Tokyo 102-8472, Japan
*Correspondence: takahama@genome.tokushima-u.ac.jp
DOI 10.1016/j.immuni.2009.10.009

SUMMARY

How self-peptides displayed in the thymus contribute to the development of immunocompetent and self-protective T cells is largely unknown. In contrast, the role of thymic self-peptides in eliminating self-reactive T cells and thereby preventing autoimmunity is well established. A type of proteasome, termed thymoproteasome, is specifically expressed by thymic cortical epithelial cells (cTECs) and is required for the generation of optimal cellularity of CD8$^+$ T cells. Here, we show that cTECs displayed thymoproteasome-specific peptide-MHC class I complexes essential for the positive selection of major and diverse repertoire of MHC class I-restricted T cells. CD8$^+$ T cells generated in the absence of thymoproteasomes displayed a markedly altered T cell receptor repertoire that was defective in both allogeneic and antiviral responses. These results demonstrate that thymoproteasome-dependent self-peptide production is required for the development of an immunocompetent repertoire of CD8$^+$ T cells.

INTRODUCTION

Most T lymphocytes are generated in the thymus. By entering the thymus and interacting with the microenvironment of the thymic cortex, lymphoid progenitor cells are induced to develop into thymocytes that express T cell receptor (TCR), as well as coreceptors CD4 and CD8 (double-positive, DP) (Scollay et al., 1988). Newly generated DP thymocytes that express a virgin set, or the germline repertoire, of TCRs are motile, seeking TCR engagement by interacting with peptide-major histocompatibility complex (MHC) expressed in the cortical microenvironment (Bousso et al., 2002; Li et al., 2007). DP thymocytes that receive weak signals of low-avidity (i.e., affinity × number per cell) TCR engagement are induced to survive and further develop into mature T cells that express large amounts of TCRs and either one of CD4 or CD8 (single-positive, SP) (Ashton-Rickardt et al., 1993, 1994; Hogquist et al., 1994; Sebzda et al., 1994; Takahama et al., 1994; Alam et al., 1996). This process is referred to as positive selection and is assumed to contribute to the enrichment of an immunocompetent, i.e., useful and self-protective, repertoire of self-MHC-restricted foreign-antigen-reactive T cells (Kisielow et al., 1988; von Boehmer, 1994; Allen, 1994; Starr et al., 2003). In contrast, DP thymocytes that receive strong signals of high-avidity TCR engagement are deleted, a process referred to as negative selection (Kappler et al., 1987; Palmer, 2003). It is well appreciated that negative selection is essential for eliminating self-reactive T cells and thereby preventing autoimmunity (Strasser, 2005; Siggs et al., 2006).

Unlike negative selection, the physiological and pathological importance of positive selection is still controversial. Positive selection was originally identified as the thymic process that determines the MHC-restriction specificity of T cells (Bevan, 1977; Zinkernagel et al., 1978) and is assumed to contribute to enriching an inherently rare T cell repertoire that is useful in the body harboring a given combination of MHC polymorphisms. However, it was shown that the germline TCR repertoire before positive and negative selection is inherently conserved to be MHC reactive (Zerrahn et al., 1997; Merkenschlager et al., 1997). It was also shown that a single MHC-peptide ligand identified in B lymphoma cells could induce positive selection of a diverse repertoire of T cells (Ignatowicz et al., 1996; Fukui et al., 1997). Based on these results, along with the structural analysis of TCR-MHC-peptide interactions, it is proposed that the specificity of TCR for peptides is not demanding during positive selection and that rather than positive selection, it is the subsequent negative selection that establishes the MHC-restriction specificity and the peptide specificity of peripheral T cells (Marrack and Kappler, 1997; Huseby et al., 2005; Dai et al., 2008; Huseby et al., 2008). However, those T cells generated in mice expressing single MHC-peptide ligands show markedly reduced cellularity and an unusual TCR repertoire that occasionally causes autoimmunity (Ignatowicz et al., 1996; Huseby et al., 2005; Oono et al., 2001). Thus, it is unclear whether the positive selection detectable in those single MHC-peptide-expressing mice represents positive selection occurring in the normal body. More importantly, it remains unanswered whether

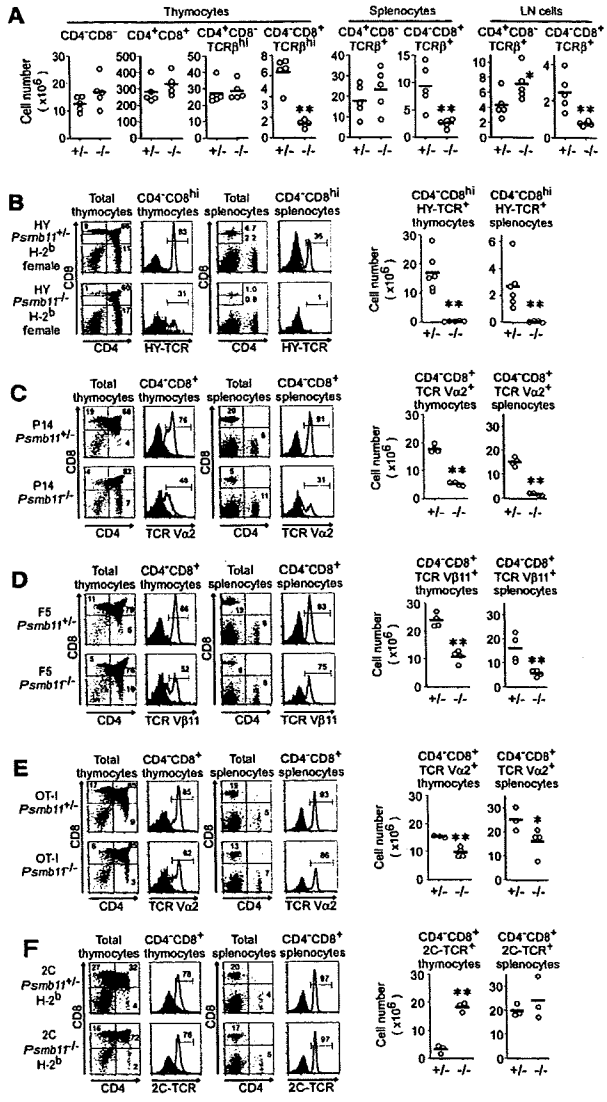

Figure 1. β5t Regulates Positive Selection of Diverse, but Not All, TCR Specificities of CD8⁺ T Cells

(A) Numbers (per mouse) of thymocytes, splenic T cells, and lymph node T cells in indicated populations were determined by flow cytometry in 3- to 6-week-old *Psmb11*$^{+/-}$ or *Psmb11*$^{-/-}$ mice. Data of individual mice (circles) and means (bars) are shown (n = 5).

(B–F) Thymocytes and splenocytes from HY-TCR-transgenic H-2^b female mice (B), as well as P14-TCR- (C), F5-TCR- (D), OT-I-TCR- (E), and 2C-TCR- (F) transgenic H-2^b mice, were analyzed by flow cytometry for CD4 and CD8. Histograms show TCR expression profiles (solid lines) obtained by staining with an antibody specific for HY-TCR (T3.70) (B), TCR Vα2 (C), TCR Vβ11 (D), TCR Vα2 (E), or 2C-TCR (1B2) (F), overlaid with control staining profiles (shaded lines), of the indicated cell populations. Numbers indicate percentage of cells within indicated areas. Graphs indicate cell numbers (per mouse) of indicated populations in individual mice (circles) and their means (bars) (n = 3 to 6). *$p < 0.05$; **$p < 0.01$. See also Figure S1.

self-peptides displayed in the thymus play a role in positive selection of an immunocompetent repertoire of T cells.

We previously identified β5t, a proteasome subunit that is specifically expressed in thymic cortical epithelial cells (cTECs) (Murata et al., 2007). Proteasomes are multicatalytic protease complexes that are responsible for the degradation of cytoplasmic proteins and the production of antigen peptides presented by MHC class I molecules (Brown et al., 1991; Rock et al., 1994). The β5 catalytic subunits of the proteasome are responsible for its chymotrypsin-like activity, producing peptides that possess at their carboxyl termini hydrophobic residues that can bind efficiently to MHC class I molecules (Heinemeyer et al., 1993; Fehling et al., 1994; Rock and Goldberg, 1999). β5t-containing proteasomes, termed thymoproteasomes, exhibit low chymotrypsin-like activity compared with the other types of proteasomes, i.e., β5-containing standard proteasomes or β5i-containing immunoproteasomes (Murata et al., 2007). Interestingly, β5t-containing cTEC-specific thymoproteasomes are essential for the generation of the optimal cellularity of CD8⁺ T cells (Murata et al., 2007). However, the mechanism by which thymoproteasomes regulate T cell development has yet to be disclosed.

In this study, we examined how thymoproteasomes regulate T cell development. Our results showed that thymoproteasomes were essential for the positive selection of major and diverse, but not all, repertoire of CD8⁺ T cells. We also found that thymoproteasomes conferred on cTECs the ability to express MHC class I -peptide complexes that were capable of generating major repertoire of CD8⁺ T cells. cTECs in thymoproteasome-deficient mice compensatively assembled immunoproteasomes and expressed an altered set of MHC class I -peptide complexes that fail to positively select most repertoires of CD8⁺ T cells. In addition, CD8⁺ T cells generated in the absence of thymoproteasomes displayed an altered TCR repertoire that was defective in allogeneic and antiviral responses. Thus, this study reveals a unique role of cTEC-specific protein degradation that is essential for the cTEC-specific production of self-peptide-MHC class I complexes, and these complexes are required for the development of an immunocompetent and self-protective repertoire of CD8⁺ T cells.

RESULTS

β5t Regulates Positive Selection of Major Repertoire of CD8⁺ T Cells

In β5t-deficient (*Psmb11*$^{-/-}$) mice, the numbers of CD8⁺ T cells in the spleen and lymph nodes were markedly reduced to 27% and 31% (ratio between averages, n = 5), respectively, of those in normal mice (Figure 1A). The number of CD4⁻CD8⁺ single-positive (CD8SP) thymocytes was also reduced to 21% (n = 5) of the control, whereas the numbers of CD4⁻CD8⁻ double-negative (DN), CD4⁺CD8⁺ DP, and CD4⁺CD8⁻ (CD4SP) thymocytes were unchanged (Figure 1A), indicating that β5t specifically regulates the CD8 lineage, but not the CD4 lineage of T cell development beyond the DP stage. Other lineages of immune cells, including TCRγδ⁺ cells, NK cells, NKT cells, macrophages, dendritic cells, B cells, and CD8αα⁺ intraepithelial lymphocytes, showed no decreases in their numbers in *Psmb11*$^{-/-}$ mice (Figure S1A available online). In order to examine how β5t specifically affects CD8⁺ T cell development, *Psmb11*$^{-/-}$ mice were crossed with TCR-transgenic mice. In HY-TCR-transgenic

mice, MHC class I H-2D^b-restricted male-antigen-specific TCR drives the positive and negative selection of CD8-lineage T cells in female and male H-2^b mice, respectively. We found that the generation of CD8SP thymocytes and splenic CD8$^+$ T cells in H-2^b female HY-TCR-transgenic mice was severely impaired by the lack of β5t (to 2.2% and 2.6%, respectively, of control cell numbers, n = 4–6) (Figure 1B). In contrast, β5t deficiency has no effect on the decreased numbers of DP thymocytes and CD8^{hi} splenic T cells in H-2^b male HY-TCR-transgenic mice (Figure S1B). Furthermore, the arrested T cell development at DP stage in null-selector H-2^d HY-TCR-transgenic mice was also unaltered by the absence of β5t (data not shown). Together, the results indicate that β5t affects positive selection rather than negative or null selection of HY-TCR-transgenic T cells. In contrast, the generation of CD4SP thymocytes and splenic CD4 T cells in I-A^b-restricted pigeon cytochrome c-specific AND-TCR-transgenic mice and I-A^b-restricted ovalbumin-specific OT-II-TCR-transgenic mice was not diminished in the absence of β5t (Figures S1F and S1G), indicating that β5t is dispensable for the positive selection of MHC class II -restricted TCR-transgenic T cells. β5t deficiency neither affected the negative selection of thymocytes in two additional MHC class I -restricted TCR-transgenic models nor caused any signs of autoimmune diseases in various organs (Figure S1C–S1E). These results indicate that the β5t-containing thymoproteasome specifically regulates positive selection, rather than negative selection, of CD8$^+$ T cells, rather than CD4$^+$ T cells.

Similar to HY-TCR-transgenic T cells, the numbers of splenic T cells in two other MHC class I -restricted TCR-transgenic mice, namely, lymphocytic choriomeningitis virus-specific P14-TCR-transgenic mice and influenza virus-specific F5-TCR-transgenic mice, were markedly reduced in the absence of β5t (12%, n = 4 and 36%, n = 4, respectively, relative to control, i.e., β5t$^+$ mice, Figures 1C and 1D). Accordingly, the generation of CD8SP thymocytes in these TCR-transgenic mice was severely impaired by the lack of β5t (Figures 1C and 1D), indicating that β5t regulates the positive selection of CD8$^+$ T cells with multiple TCR specificities. Interestingly, however, MHC class I -restricted ovalbumin-specific OT-I-TCR-transgenic and allogeneic H-2L^d-specific 2C-TCR-transgenic CD8$^+$ T cells were less severely affected in *Psmb11*$^{-/-}$ mice (Figures 1E and 1F). The number of OT-I-TCR-transgenic splenic CD8$^+$ T cells in *Psmb11*$^{-/-}$ mice was reduced to 64% (n = 3 to 4) of that in control OT-I-TCR-transgenic mice (Figure 1E). Most notable was that the number of 2C-TCR-transgenic splenic CD8$^+$ T cells in *Psmb11*$^{-/-}$ mice was 122% (n = 3) of that in control 2C-TCR-transgenic mice carrying β5t (Figure 1F). These results indicate that the development of CD8$^+$ T cells that express individual specificities of MHC class I -restricted TCRs is differentially dependent on β5t. Along with the finding that the majority of CD8$^+$ T cells are lost in *Psmb11*$^{-/-}$ mice (Figure 1A), these results also indicate that the β5t-containing thymoproteasome regulates the positive selection of major and diverse, but not all, repertoires of MHC class I -restricted CD8$^+$ T cells.

β5t Regulates cTEC-Mediated Positive Selection of CD8$^+$ T Cells within Thymic Cortex

To determine the cells that are responsible for the β5t-mediated regulation of T cell development, we examined positive selection among various TCR specificities in bone marrow chimeras (Figure 2A). To do so, hematopoietic progenitor cells from TCR-transgenic mice were reconstituted in irradiated *Psmb11*$^{-/-}$ mice. In the thymus of β5t-deficient mice, positive selection of HY-TCR-, P14-TCR-, and F5-TCR-transgenic T cells was markedly diminished, whereas positive selection of OT-I-TCR-transgenic and 2C-TCR-transgenic T cells was affected little (Figure 2A). Thus, the differential β5t dependence of positive selection among various TCR specificities was reproduced in these bone marrow chimeras reconstituted in the thymus of irradiated *Psmb11*$^{-/-}$ mice (Table 1). In contrast, β5t deficiency in bone marrow donor cells did not diminish the positive selection of HY-TCR-transgenic T cells in the thymus of β5t-sufficient mice (Figure 2A), indicating that β5t in nonhematopoietic stromal cells, but not bone marrow-derived hematopoietic cells, is responsible for positive selection of the repertoire of CD8SP thymocytes. Furthermore, the specific deficiency of β5t in cTEC-enriched thymic stromal cells markedly diminished the capability to induce the generation of CD8$^+$ T cells from isolated DP thymocytes of P14-TCR-transgenic mice, but not 2C-TCR-transgenic mice, in reaggregated fetal thymus organ culture (Figure 2B). Along with the results showing that β5t is exclusively expressed in cTECs (Murata et al., 2007 and data not shown), these results indicate that thymoproteasome-expressing cTECs regulate the positive selection of major and diverse, but not all, repertoire of CD8$^+$ T cells. The β5t independency of positive selection weakly correlated with the signaling intensity of transgenic TCR, which was measured by the amount of surface CD5 and CD8 expression (Figure S5).

In thymic medulla, newly generated SP thymocytes interact with various cells, including mTECs, which promiscuously express various tissue-specific antigens (Derbinski et al., 2001; Anderson et al., 2002; Kyewski and Derbinski, 2004). The CCR7-mediated migration of SP thymocytes to the medulla is essential to trim the cortically generated T cell repertoire to establish self-tolerance (Takahama, 2006; Kurobe et al., 2006; Nitta et al., 2009). Thus, it is possible that the β5t regulation of repertoire formation may involve the migration of positively selected thymocytes to the medulla and the negative selection induced in thymic medulla. However, we found that the development of CD8SP thymocytes was defective even in *Psmb11*$^{-/-}$ *Ccr7*$^{-/-}$ mice, similar to *Psmb11*$^{-/-}$ mice (Figure 2C), indicating that defective positive selection in the absence of β5t reflects neither CCR7-mediated migration of positively selected thymocytes nor negative selection in thymic medulla. We also found that the formation of thymic medulla including Aire-expressing medullary epithelial cells was not impaired in β5t-deficient mice (Figure S2). Thus, β5t-containing thymoproteasome regulates the positive selection of major CD8$^+$ T cell repertoires within thymic cortex without the contribution of subsequent negative selection in thymic medulla.

The reduced number of CD8$^+$ T cells in bone marrow chimeras reconstituted in irradiated *Psmb11*$^{-/-}$ mice was not markedly altered when bone marrow cells were isolated from mice deficient for β2-microglobulin (β2 m), a component of MHC class I molecules (Figure 2D). Thus, the impaired but detectable positive selection in β5t-deficient mice is not due to MHC class I -restricted antigen presentation by bone marrow-derived cells, including dendritic cells and T-lineage cells, which were

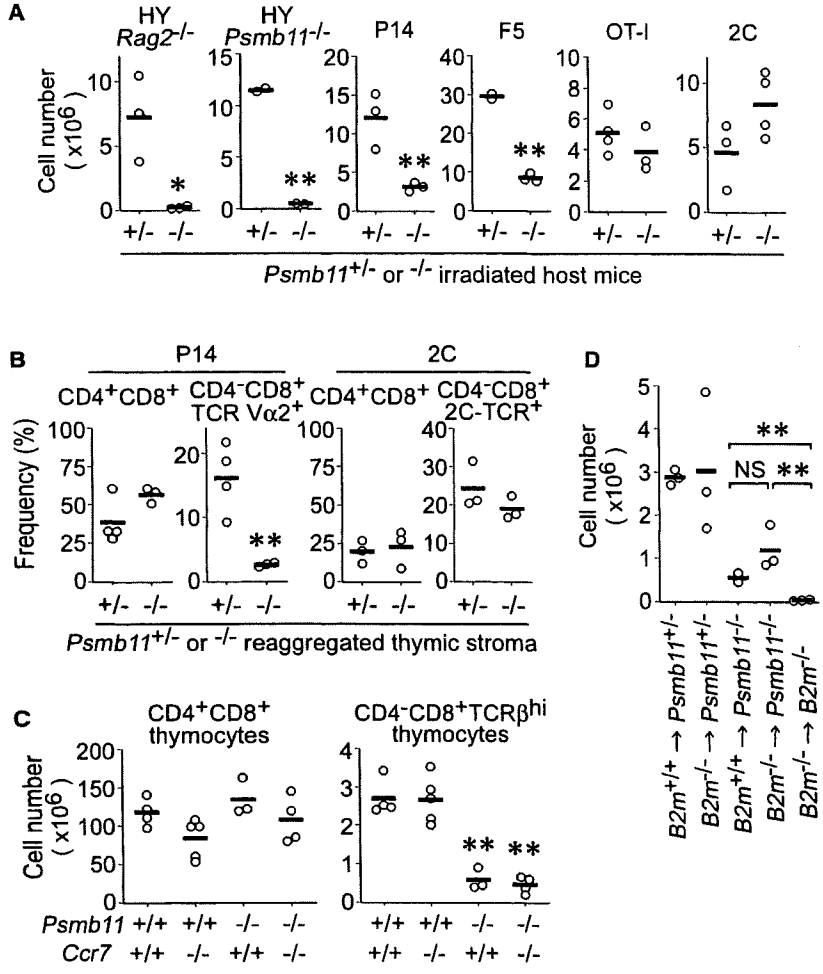

Figure 2. β5t in cTECs Regulates Positive Selection of Major TCR Specificities of CD8⁺ T Cells

(A) T cell-depleted bone marrow cells from indicated donor mice were transferred into lethally irradiated *Psmb11*$^{+/-}$ or *Psmb11*$^{-/-}$ H-2^{b} host mice. Thymocytes were analyzed 5 weeks after the reconstitution. Graphs indicate numbers (per mouse) of CD4^{-}CD8^{+}TCR^{hi} thymocytes in individual mice (circles) and their means (bars) (n = 2 to 4).

(B) CD4^{+}CD8^{+} thymocytes were isolated from P14-TCR-transgenic (left) or 2C-TCR-transgenic (right) mice with a cell sorter and reaggregated with *Psmb11*$^{+/-}$ or *Psmb11*$^{-/-}$ H-2^{b} fetal thymic stromal cells that contained 30%–40% cTECs, <3% mTECs, and 60%–70% non-TEC stromal cells, isolated from 2-deoxyguanosine-treated fetal thymus lobes. CD4^{+}CD8^{+} thymocytes before the culture had > 99% purity. The indicated cell populations were analyzed 4 days after reaggregated thymus organ culture. Graphs indicate percentages of indicated populations in individual reaggregated thymuses (circles) and their means (bars) (n = 3 to 4).

(C) Numbers of CD4^{+}CD8^{+} or CD4^{-}CD8^{+}TCRβ^{hi} thymocytes (per thymus lobe) in 4- to 6-week-old *Psmb11*$^{+/+}$*Ccr7*$^{+/+}$, *Psmb11*$^{+/+}$*Ccr7*$^{-/-}$, *Psmb11*$^{-/-}$*Ccr7*$^{+/+}$, or *Psmb11*$^{-/-}$*Ccr7*$^{-/-}$ mice.

(D) Thymocytes isolated from indicated bone marrow chimera mice were analyzed by flow cytometry for the expression of CD4, CD8, and TCRβ. Shown are the numbers of CD4^{-}CD8^{+}TCRβ^{high} thymocytes (n = 2 to 3). The number of CD8SP thymocytes in *Psmb11*$^{-/-}$ mice reconstituted with *B2m*$^{-/-}$ bone marrow cells (*B2m*$^{-/-}$ → *Psmb11*$^{-/-}$) was not significantly ($p \geq 0.05$) different from that in *Psmb11*$^{-/-}$ mice reconstituted with *B2m*$^{+/+}$ bone marrow cells (*B2m*$^{+/+}$ → *Psmb11*$^{-/-}$) but was significantly ($p < 0.01$) larger than that in *B2m*$^{-/-}$ mice reconstituted with *B2m*$^{-/-}$ bone marrow cells (*B2m*$^{-/-}$ → *B2m*$^{-/-}$), indicating that the generation of CD8SP thymocytes in *Psmb11*$^{-/-}$ mice was independent of bone-marrow-derived MHC class I molecules. *$p < 0.05$; **$p < 0.01$; NS, not significant. See also Figure S2.

previously shown to be capable of inducing positive selection under certain experimental conditions (Zinkernagel and Althage, 1999; Li et al., 2005; Choi et al., 2005; Kirberg et al., 2008). Rather, the reduced production of CD8^{+} T cells in *Psmb11*$^{-/-}$ mice is likely due to the defective and inefficient capability of thymoproteasome-deficient cTECs to induce positive selection.

cTECs Display a Thymoproteasome-Specific Set of MHC Class I-Associated Peptides

The surface expression of H-2K and H-2D MHC class I molecules, as well as I-A MHC class II molecules, on cTECs in *Psmb11*$^{-/-}$ mice was not markedly diminished (Figure 3A), although the surface expression of K^{b}, D^{b}, and L^{d} on β5t-deficient cTECs was slightly altered to 93% (n = 5), 89% (n = 5), and 103% (n = 3) of that in control cTECs carrying β5t (Table 2). Similar to cTECs from normal mice, β5t-deficient cTECs were fully capable of presenting SIINFEKL antigen peptide to stimulate OT-I-TCR-transgenic CD8^{+} T cells (Figure 3B). Thus, β5t-deficient cTECs are competent in presenting antigen peptides to MHC class I -restricted T cells. The majority of proteasomal β5-type subunits expressed in β5t-deficient cTECs were β5i, rather than β5 (Figure 3C), whereas β1i and β2i, rather than β1 or β2, were predominant in cTECs (Murata et al., 2007). Thus, unlike normal cTECs that predominantly express β5t-containing thymoproteasomes, β5t-deficient cTECs compensatively assemble β1i-, β2i-, and β5i-containing immunoproteasomes. Indeed, most MHC class I H-2L^{d} molecules expressed by cTECs exhibited the peptide-bound "folded" form (as detected by 30-5-7 antibody), rather than the peptide-empty "open" form (as detected by 64-3-7 antibody), irrespective of the presence or absence of β5t (Figure 3D). Thus, most MHC class I molecules expressed by cTECs in the presence or absence of β5t are associated with peptides, similarly to those expressed by other cells, such as mTECs.

In order to explore the nature of MHC class I -associated peptides in cTECs, we then examined the expression of epitopes

Table 1. Development of CD8$^+$ T Cells that Express Individual Specificities of MHC Class I -Restricted TCR Is Differentially Dependent on β5t

				% *Psmb11*$^{-/-}$/*Psmb11*$^{+/-}$[b]			
		MHC	Antigen	Thymocytes		Splenocytes	
TCR	Vα and Vβ	Restriction	Peptide[a]	Mice[c]	BMC[c]	Mice	BMC
Bulk	Bulk	Bulk	Bulk	21.0	19.6	27.3	17.8
HY	Vα17 Vβ8.2	D^b	Smcy	2.2	3.7	2.6	5.8
P14	Vα2 Vβ8.1	D^b	LCMV gp33	29.7	26.1	12.4	12.3
F5	Vα4 Vβ11	D^b	Flu NP68	45.3	28.9	35.5	14.9
OT-I	Vα2 Vβ5	K^b	Ovalbumin	63.4	76.0	63.9	56.0
2C[d]	Vα3 Vβ8.2	K^b	(L^d + α-KGDH)	553.2	181.1	121.7	47.7

[a] Smcy is a Y-chromosome-encoded H-Y antigen. LCMV gp33 is glycoprotein 33 of lymphocytic choriomeningitis virus. Flu NP68 is influenza virus nucleoprotein 68.
[b] 100 × (average CD8$^+$ SP T cell number in *Psmb11*$^{-/-}$ mice/average CD8$^+$ SP T cell number in *Psmb11*$^{+/-}$ mice).
[c] Mice, data obtained from TCR-transgenic mice as shown in Figure 1. BMC, data from bone marrow chimera mice as shown in Figure 2A.
[d] 2C-TCR-transgenic T cells in H-2^b mice are positively selected by K^b and are reactive to allogeneic L^d molecules that are associated with the endogenous protein α-ketoglutarate dehydrogenase (α-KGDH).

produced by the complexes of MHC class I molecules and limited varieties of peptides. We found that the expression of one of these epitopes directly detected by the TCR-like monoclonal antibody 25-D1.16 (Porgador et al., 1997; Mareeva et al., 2008), which recognizes a fraction of H-2K^b molecules associated with a population of peptides (Porgador et al., 1997), was markedly higher in cTECs from *Psmb11*$^{-/-}$ mice than in those from control mice (Figures 3E–3G). The surface expression of this epitope on mTECs, thymocytes, B cells, and dendritic cells was not different between *Psmb11*$^{-/-}$ and control mice (Figures 3E and 3F and Figure S3A), indicating that β5t specifically regulates the surface expression of this epitope on cTECs. Likewise, the cell-surface expression of another epitope of the H-2K^b complex associated with a different population of peptides, detected by 22-C5.9 (Porgador et al., 1997), was specifically altered in cTECs from *Psmb11*$^{-/-}$ mice compared to those from control mice (Table 2 and Figure S3B). The cTEC-specific difference in the expression of these epitopes between *Psmb11*$^{-/-}$ and control mice suggests that the repertoire of MHC class I -associated peptides expressed by cTECs is specifically regulated by β5t-containing thymoproteasomes and that cTECs in normal mice display a repertoire of MHC class I-associated peptides that are uniquely generated by thymoproteasomes.

Functionally Incompetent Repertoire of CD8$^+$ T Cells in β5t-Deficient Mice

Finally, we examined the function and repertoire of lymphopenic CD8$^+$ T cells that were generated in the absence of β5t. We found that CD8$^+$ T cells generated in *Psmb11*$^{-/-}$ mice were capable of proliferation and granzyme B production in response to TCR and CD28 stimulation (Figures 4A and 4B). OT-I-TCR-transgenic CD8$^+$ T cells generated in *Psmb11*$^{-/-}$ mice were fully capable of proliferating in the presence of SIINFEKL peptide (Figure 4C). Homeostatic proliferation of CD8$^+$ T cells isolated from *Psmb11*$^{-/-}$ mice was not impaired in vivo in both irradiated mice and RAG2-deficient (*Rag2*$^{-/-}$) mice (Figure 4D). Thus, CD8$^+$ T cells generated in the absence of thymoproteasomes are functionally potent to maintain in vivo survival in lymphopenic environments and to proliferate and become cytotoxic T-lymphocytes (CTL) in response to TCR stimulation.

CD8$^+$ T cells in *Psmb11*$^{-/-}$ mice exhibited increased frequency of cells that highly expressed CD44 and Ly6C (Figure 4E). The frequency of CD44^{hi} CD8$^+$ T cells in *Psmb11*$^{-/-}$ mice increased with the ontogeny (Figure 4F) and this increase coincided with the severer decrease in absolute number of CD44^{lo} CD8$^+$ T cells than CD44^{hi} CD8$^+$ T cells (Figure 4G). Both CD44^{lo} and CD44^{hi} CD8$^+$ T cells in *Psmb11*$^{-/-}$ mice were capable of proliferative response to TCR and CD28 stimulation (Figure 4H). However, CD44^{lo} CD8$^+$ T cells isolated from wild-type mice did not undergo excessive homeostatic expansion upon intravenous administration in *Psmb11*$^{-/-}$ mice, unlike in lymphopenic *Rag2*$^{-/-}$ mice (Figure 4I), suggesting that the increase in frequency of CD44^{hi} cells is unlikely due to the homeostatic expansion of CD44^{lo} cells and subsequent phenotype conversion into CD44^{hi} cells in *Psmb11*$^{-/-}$ mice. Thus, the marked in vivo persistence of CD44^{hi} memory-type CD8$^+$ T cells compared to CD44^{lo} naive CD8$^+$ T cells (Tanchot et al., 1997; Murali-Krishna et al., 1999) and possible defect in the maintenance of CD8$^+$ T cells generated in *Psmb11*$^{-/-}$ mice (for example, by defective TCR interactions with self MHC class I-peptide complexes because of the alteration in TCR repertoire) may contribute to the increased ratio of CD44^{hi} cells over CD44^{lo} cells in CD8$^+$ T cells of *Psmb11*$^{-/-}$ mice and the slightly elevated responses of CD8$^+$ T cells from *Psmb11*$^{-/-}$ mice.

Indeed, the distribution of TCR-Vβ and TCR-Vα in CD8$^+$ T cells was altered in *Psmb11*$^{-/-}$ mice (Figure 5A), whereas no substantial difference was detected in the TCR-V distribution in CD4$^+$ T cells between *Psmb11*$^{-/-}$ and control mice (Figure 5A), indicating that the T cell repertoire was altered specifically in CD8$^+$ T cells. Thus, CD8$^+$ T cells generated in *Psmb11*$^{-/-}$ mice carry undiminished TCR responsiveness but an altered TCR repertoire. The functional consequence of the altered repertoire of CD8$^+$ T cells in *Psmb11*$^{-/-}$ mice was examined by measuring immune response to foreign antigens. We found that CD8$^+$ T cells isolated from *Psmb11*$^{-/-}$ mice showed markedly diminished proliferative responses to allogeneic antigens (Figure 5B), which were dependent on β2 m-associated MHC class I

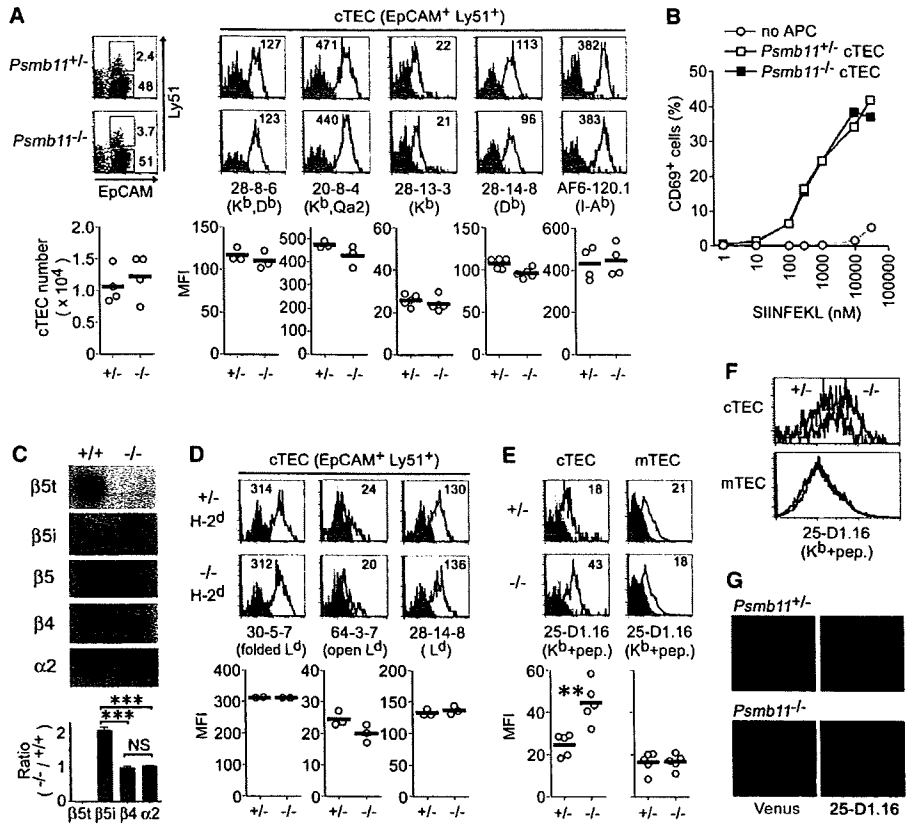

Figure 3. cTECs Produce β5t-Specific Peptide-MHC Class I Complexes

(A) Surface expression of MHC class I and class II molecules on cTECs from *Psmb11*$^{+/-}$ or *Psmb11*$^{-/-}$ H-2^{b} mice. CD45^{-}TER119^{-} thymic stromal cells from 2-week-old mice were stained for EpCAM, Ly51, and indicated antibodies specific for MHC class I or class II molecules. Histograms show staining profiles (solid lines) overlaid with control staining profiles (shaded histograms) of EpCAM^{+}Ly51^{+} cTECs. Numbers in histograms indicate mean fluorescence intensity (MFI). Graphs show MFI of the histograms with indicated antibodies in individual measurements (circles) and their means (bars). Shown on the left are representative dot plots for EpCAM and Ly51 expression in CD45^{-} thymic stromal cells and the number of EpCAM^{+}Ly51^{+} cTECs in *Psmb11*$^{+/-}$ or *Psmb11*$^{-/-}$ mice. Numbers in dot plots indicate the frequency of cells within the box. The expression of D^{b} was significantly ($p < 0.05$) reduced in *Psmb11*$^{-/-}$ mice.

(B) CD8^{+} T cells from the spleen of OT-I-TCR-transgenic mice were cocultured in the absence or presence of CD45^{-}I-A^{+}Ly51^{+} cTECs from *Psmb11*$^{+/-}$ or *Psmb11*$^{-/-}$ H-2^{b} mice. cTECs were pretreated with indicated concentrations of SIINFEKL peptide. Twenty hours later, the frequency of CD69^{+} cells in CD8^{+} T cells was analyzed by flow cytometry.

(C) Proteasomal components in β5t-deficient cTECs. Ly51^{+} cells were purified from the thymus of *Psmb11*$^{+/-}$ or *Psmb11*$^{-/-}$ mice, lysed, and subjected to immunoblot analysis with the indicated antibodies. β4 and α2 were used as controls. Means and standard errors ($n = 3$) of the ratios of the chemiluminescence signals in *Psmb11*$^{-/-}$ cTECs to those in *Psmb11*$^{+/+}$ cTECs are also shown. ***$p < 0.001$; NS, not significant. The signals for β5 were not detectable in cTECs from either *Psmb11*$^{+/+}$ or *Psmb11*$^{-/-}$ mice.

(D–F) CD45^{-}TER119^{-} thymic stromal cells were prepared from 2-week-old *Psmb11*$^{+/-}$ or *Psmb11*$^{-/-}$ H-2^{d} (D) or H-2^{b} (E) mice (F) and stained for EpCAM, Ly51, and indicated MHC class I molecules. Monoclonal antibodies used were 30-5-7 (specific for the peptide-bound "folded" form of L^{d}), 64-3-7 (specific for the peptide-empty "open" form of L^{d}), 28-14-8 (specific for L^{d} irrespective of peptide binding), and 25-D1.16 (specific for K^{b} associated with a limited variety of peptides). Histograms show staining profiles (solid lines) overlaid with control staining profiles (shaded histograms) of EpCAM^{+}Ly51^{+} cTECs or EpCAM^{+}Ly51^{-} mTECs (D and E). Staining profiles of EpCAM^{+}Ly51^{+} cTECs and EpCAM^{+}Ly51^{-} mTECs isolated from *Psmb11*$^{-/-}$ (red lines) and *Psmb11*$^{+/-}$ (black lines) mice are also indicated (F). Numbers in histograms indicate MFI. Graphs show the MFI of the histograms with indicated antibodies in individual measurements (circles) and their means (bars). **$p < 0.01$.

(G) Venus-expressing (green) cTECs isolated from β5t$^{+/-}$ or β5t$^{-/-}$ H-2^{b} mice were stained with 25-D1.16 (red).

See also Figure S3.

molecules (Figure 5C). The decrease in allogeneic response was not limited to a single combination of allogeneic stimulation but was shared by various allogeneic combinations (Figures 5B and 5C and Figure S4A). However, a certain combination of allogeneic response (H-2^{d} anti-H-2^{bq4}) of CD8^{+} T cells was not severely defective in *Psmb11*$^{-/-}$ mice (Figure S4A), in agreement with the possibility that CD8^{+} T cells generated in the absence of thymoproteasomes are functionally potent in response to TCR engagement but are defective in the formation of a functionally competent TCR repertoire. The allogeneic response of CD8^{+} T cells from *Psmb11*$^{-/-}$ mice was reduced even in isolated CD44^{lo} naive T cells (Figure S4B), suggesting that the defective

Table 2. Surface Expression of MHC Molecules on cTECs and mTEC in β5t-Deficient Mice

Mouse Examined	Target Molecule	Detecting Antibody	% *Psmb11*$^{-/-}$/*Psmb11*$^{+/-}$[a]	
			cTECs	mTECs
H-2^b	K^b, D^b	28-8-6	94.4	101.5
	K^b, Qa2	20-8-4	89.9	93.5
	K^b	28-13-3	93.4	105.0
	D^b	28-14-8	89.1	100.1
	K^b + peptides[b]	25-D1.16	180.2[b]	101.3
	K^b + peptides[b]	22-C5.9	139.1[b]	95.4
	I-A^b	AF6-120.1	103.3	102.6
H-2^d	L^d	28-14-8	102.8	100.3
	L^d (folded)[c]	30-5-7	99.8	95.6
	L^d (open)[c]	64-3-7	81.5	92.0

[a] MFI values of indicated molecules with indicated antibodies were measured by flow cytometry as shown in Figure 3. Shown are 100 × (average MFI in *Psmb11*$^{-/-}$ mice/average MFI in *Psmb11*$^{+/-}$ mice). For the analysis with 22-C5.9, cTECs and mTECs were *Psmb11*-driven Venus$^+$ and Venus$^-$ CD45$^-$ thymic cells.

[b] 25-D1.16 and 22-C5.9 are specific for K^b associated with a limited and mutually different variety of peptides (Porgador et al., 1997). The MFI values were significantly ($p < 0.05$) larger in *Psmb11*$^{-/-}$ cTECs than in *Psmb11*$^{+/-}$ cTECs.

[c] 30-5-7 is specific for the peptide-bound folded form of L^d, whereas 64-3-7 is specific for the peptide-empty open form of L^d (Lie et al., 1991).

CD8$^+$ T cell response in *Psmb11*$^{-/-}$ mice is due to the defective repertoire of naive CD8$^+$ T cells rather than the reduced frequency of naive cells in CD8$^+$ T cells. Finally, we found that upon influenza virus infection under the conditions where control mice could survive due to CD8$^+$ T cell responses, *Psmb11*$^{-/-}$ mice exhibited severe lethality (Figure 5D). These results indicate that CD8$^+$ T cells generated in the absence of thymoproteasomes are defective in mounting immune responses to allogeneic and viral antigens.

DISCUSSION

The present results demonstrate that cTECs display thymoproteasome-specific MHC class I-peptide complexes that are essential for the development of major and diverse repertoire of CD8$^+$ T cells. Thymoproteasome-deficient cTECs displayed altered MHC class I-peptide complexes that generated an altered TCR repertoire that was defective in allogeneic and antiviral responses. These results suggest that cTEC-specific production of MHC class I-associated self-peptides due to thymoproteasome-mediated protein degradation is essential for the development of an immunocompetent and self-protective CD8$^+$ T cell repertoire.

Chymotrypsin-like activity mediated by the β5 subunits of proteasomes is responsible for the production of peptides that carry carboxyl-terminal hydrophobic residues that efficiently associate with MHC class I molecules (Fehling et al., 1994; Rock and Goldberg, 1999). No carboxypeptidases other than proteasomes are detectable in the cells except lysosomes, whereas various aminopeptidases in the cytoplasm and the endoplasmic reticulum are involved in trimming the amino termini of proteasome-generated peptides (Reits et al., 2003; Yewdell et al., 2003). Indeed, naturally processed self-peptides eluted from many alleles of MHC class I molecules are highly biased to possess hydrophobic amino acids, and basic residues to a less extent, at the carboxyl terminus (Falk et al., 1991; Hunt et al., 1992; Young et al., 1995). On the other hand, β5t-containing thymoproteasomes exhibit selectively reduced chymotrypsin-like activity but normal trypsin-like and caspase-like activities, compared with other types of proteasomes, i.e., β5-containing standard proteasomes and β5i-containing immunoproteasomes (Murata et al., 2007). It is therefore reasonable to speculate that the specifically reduced chymotrypsin-like activity in thymoproteasomes is responsible for the generation of the cTEC-specific repertoire of cytoplasmic peptides. Even though the TAP complex, which is responsible for transporting cytoplasmic peptides into the lumen of the endoplasmic reticulum, prefers the hydrophobic carboxyl termini of the peptides (Momburg et al., 1994; Uebel et al., 1997; Burgevin et al., 2008), our results show that most of the MHC class I molecules expressed on the surface of cTECs irrespective of β5t expression are associated with the peptides rather than being peptide-empty. Thus, the thymoproteasome-mediated production of a cTEC-specific repertoire of cytoplasmic peptides likely results in the production of a unique repertoire of MHC class I-associated peptides specifically displayed by cTECs.

With regard to the nature of MHC class I-bound peptides expressed by cTECs, current technology of mass spectrometry analysis (which requires 10^8 to 10^9 cells) does not readily allow us to directly identify the sequences of MHC-bound peptides expressed by isolated cTECs (approximately 1×10^4 cells can be isolated per mouse). However, the present results obtained by the two different TCR-like monoclonal antibodies show that the expression of the epitopes, likely produced by the complexes of MHC class I molecules and endogenously produced peptides, was markedly and specifically altered in cTECs from β5t-deficient mice compared to those from control mice, suggesting that cTECs display a thymoproteasome-specific set of MHC class I-associated peptides. The peptides expressed by cTECs may be unique to cTECs and different from the peptides expressed by other cells because of the unique enzymatic activity of cTEC-specific thymoproteasome. Alternatively, the decreased chymotrypsin-like activity of thymoproteasomes may uniquely limit the variety of MHC class I-associated peptides displayed by cTECs. It is also possible that these antibodies may recognize a conformational status of K^b, which may be increased specifically in cTECs in the absence of β5t but be independent of the variety of associated peptides.

Our results show that the positive selection of various transgenic TCR is differentially affected by β5t deficiency in multiple magnitudes rather than in an all-or-none manner. It is thus speculated that the positive selection of a single TCR specificity is induced by multiple (thymoproteasome-dependent and thymoproteasome-independent) peptides associated with MHC class I molecules. A major fraction of positively selecting peptides may be uniquely generated by thymoproteasomes in cTECs, whereas some positively selecting peptides may be additionally generated in a thymoproteasome-independent manner.

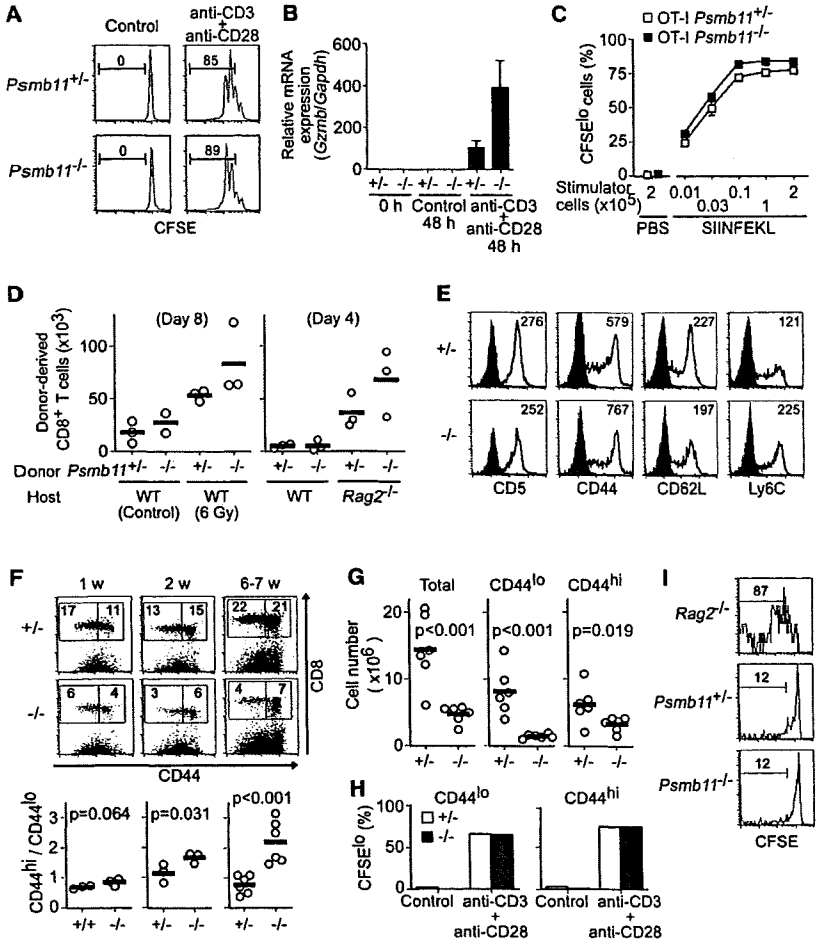

Figure 4. CD8$^+$ T Cells Generated in β5t-Deficient Mice Are Functionally Potent to Proliferate and Become Cytotoxic T-Lymphocytes in Response to TCR Stimulation In Vitro and to Maintain Survival In Vivo

(A and B) Splenic CD8$^+$ T cells were purified from *Psmb11*$^{+/-}$ or *Psmb11*$^{-/-}$ mice, labeled with CFSE, and cultured with or without plate-bound anti-CD3 and anti-CD28 for 48 hr. (A) Histograms show CFSE fluorescence profiles, and numbers indicate the frequency of CFSE^{lo} cells. (B) mRNA expression of granzyme B determined by quantitative RT-PCR analysis was normalized to GAPDH mRNA expression, and those in *Psmb11*$^{+/-}$ CD8$^+$ T cells before the culture were set to 1.

(C) Splenic CD8$^+$ T cells (1×10^5) from *Psmb11*$^{+/-}$ or *Psmb11*$^{-/-}$ OT-I-TCR-transgenic H-2^b mice were labeled with CFSE and cultured with PBS- or SIINFEKL-loaded C57BL/6 splenocytes for 40 hr. Graphs show means ± standard errors of the frequency of CFSE^{lo} cells (n = 3).

(D) Splenic CD8$^+$ T cells from *Psmb11*$^{+/-}$ or *Psmb11*$^{-/-}$ mice were labeled with CFSE and intravenously injected into nonirradiated (control) or irradiated (6 Gy) wild-type mice or nonirradiated *Rag2*$^{-/-}$ mice (1×10^6 cells/host mouse). Graphs indicate numbers of CD8$^+$CFSE$^+$ splenocytes in individual mice (circles) and their means (bars) (n = 2 to 3).

(E) The expression of CD5, CD44, CD62L, and Ly6C in CD8$^+$TCRβ$^+$ spleen cells from β *Psmb11*$^{+/-}$ or *Psmb11*$^{-/-}$ mice was analyzed by flow cytometry. Numbers in histograms indicate MFI.

(F) The expression of CD44 and CD8 in TCRβ$^+$ spleen cells from *Psmb11*$^{+/-}$ or *Psmb11*$^{-/-}$ mice at indicated ages was analyzed by flow cytometry. Numbers in dot plots indicate the frequency of cells within the box. Graphs indicate the ratios of the numbers of CD44^{hi} CD8$^+$ T cells over CD44^{lo} CD8$^+$ T cells in individual mice (circles) and their means (bars, n = 3–6). *p < 0.05.

(G) Absolute numbers (circles) and their means (bars, n = 6) of total, CD44^{lo}, and CD44^{hi} subsets of CD8$^+$TCRβ$^+$ spleen cells in *Psmb11*$^{+/-}$ or *Psmb11*$^{-/-}$ mice at 6 to 7 weeks old were analyzed by flow cytometry.

(H) CD44^{lo} and CD44^{hi} CD8$^+$ T cells isolated from the spleen of *Psmb11*$^{+/-}$ (open bars) or *Psmb11*$^{-/-}$ (closed bars) mice were labeled with CFSE and cultured with or without plate-bound anti-CD3 and anti-CD28 antibodies for 48 hr. Graphs indicate the frequency of CFSE^{lo} cells.

(I) CD44^{lo} CD8$^+$ T cells (5×10^6) from wild-type mice were CFSE-labeled and intravenously administered into nonirradiated *Rag2*$^{-/-}$, *Psmb11*$^{+/-}$, or *Psmb11*$^{-/-}$ mice. Histograms show representative CFSE fluorescence profiles (n ≥ 5), and numbers indicate the frequency of CFSE^{lo} cells.

It is also interesting to note that the signaling intensity of transgenic TCR, which is measured by the amount of surface CD5 and CD8 expression (Park et al., 2007), weakly correlated with the presumable β5t independency of positively selecting ligands, suggesting that positively selecting peptides generated in cTECs by thymoproteasomes tend to exhibit low TCR signaling intensity. It is possible that the MHC class I -associated self-peptides uniquely displayed by cTECs may be rich in peptides that exhibit low-avidity TCR engagement, as previously suggested (Ashton-Rickardt et al., 1994). It should be emphasized that the order of β5t independency among the TCR-transgenic models (HY < P14 < F5 < OT-I < 2C) is not identical to the order of the TCR signaling intensity (HY < F5 < 2C ≤ P14 < OT-I) (Figure S5; Ernst et al., 1999; Ge et al., 2004; Park et al., 2007; Agenès et al., 2008), arguing against the possibility that β5t regulates the production or activity of a general costimulus for positive selection. Indeed, our results showing that β5t-deficient cTECs are fully capable of presenting various concentrations of antigen peptide to stimulate CD8$^+$ T cells contradict such possibility.

The present results also show that β5i-containing immunoproteasomes appear to be the dominant cellular proteasome in cTECs of β5t-deficient mice. Immunoproteasomes are able to produce a set of peptides that efficiently associate with MHC class I molecules at the carboxyl terminus (Rock and Goldberg, 1999). Indeed, our results suggest that cTECs in β5t-deficient mice express the MHC class I -peptide complex, whereas the altered set of MHC class I-peptide complex expressed by thymoproteasome-deficient and thereby immunoproteasome-dominant cTECs is inefficient in inducing the positive selection of major CD8$^+$ T cell repertoires. Thus, in order to generate an optimum CD8$^+$ T cell repertoire, cTECs may have to display a repertoire of MHC class I-bound peptides that inefficiently

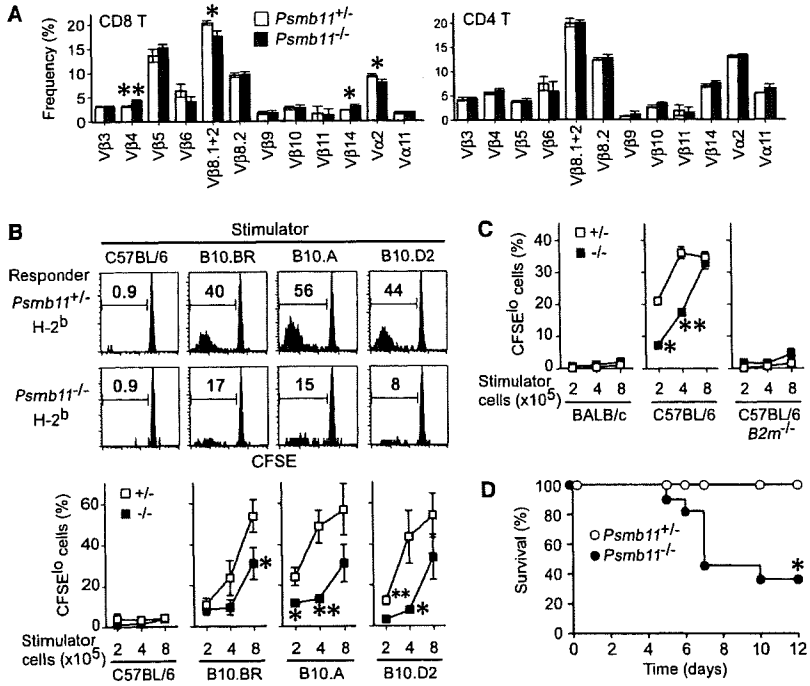

Figure 5. Altered TCR Repertoire and Defective Immune Responses of CD8⁺ T Cells in β5t-Deficient Mice

(A) TCR-Vβ and TCR-Vα distribution in $CD8^+TCR\beta^+$ spleen cells ($CD8^+$ T cells) or $CD8^-TCR\beta^+$ spleen cells (CD4 T cells) from *Psmb11*$^{+/-}$ or *Psmb11*$^{-/-}$ mice was determined by flow cytometry. Graphs show means ± standard errors of three independent measurements.

(B and C) Splenic $CD8^+$ T cells (1×10^5) from *Psmb11*$^{+/-}$ or *Psmb11*$^{-/-}$ H-2^b (B) or H-2^d (C) mice were labeled with CFSE and cocultured with irradiated splenocytes ($2 \times$, $4 \times$, or 8×10^5) from indicated mouse strains for 4 days. Histograms show representative CFSE fluorescence profiles of $CD8^+$ T cells cultured with 4×10^5 stimulator cells. Numbers in histograms indicate the frequency of $CFSE^{lo}$ cells. Graphs show means ± standard errors of at least three independent measurements.

(D) Eleven *Psmb11*$^{-/-}$ mice (closed circles) and 6 *Psmb11*$^{+/-}$ mice (open circles) were infected with 1,000 PFU of A/PR8 virus. Survival was monitored up to 12 days after the infection. Data were pooled from two experiments. The Mann-Whitney nonparametric *U*-test was used to compare survival between groups of mice. $^*p < 0.05$; $^{**}p < 0.01$.

See also Figure S4.

associate with MHC class I molecules and tend to provide low TCR signaling intensity.

Our results show that $CD8^+$ T cells in β5t-deficient mice are defective in allogeneic and antiviral responses. Upon TCR stimulation, $CD8^+$ T cells in β5t-deficient mice were capable of proliferation and granzyme B production. On the other hand, the TCR repertoire in V regions of $CD8^+$ T cells was altered in β5t-deficient mice. Allogeneic responses of $CD8^+$ T cells in β5t-deficient mice were defective in various, but not all, allogeneic combinations and were defective even when $CD8^+$ T cells were isolated into naive T cells. Thus, we think that the defect in immune responses of β5t-deficient mice is due to an altered repertoire of $CD8^+$ T cells generated in the absence of β5t-containing thymoproteasome. It is remarkable that the thymoproteasome, which may affect the MHC class I-associated peptide repertoire specifically in cTECs, is essential for shaping the immunocompetent TCR repertoire of $CD8^+$ T cells.

We found that the immune protection of β5t-deficient mice from influenza virus infection is defective. Cytotoxic T lymphocyte (CTL) activity was observed in mice from day 5 to day 15 after influenza virus infection (Kedzierska et al., 2006; Stambas et al., 2007) and that virus-specific CD8 CTLs are the key effectors of virus clearance in mice infected with influenza virus (Bender et al., 1992; Mozdzanowska et al., 1997; Doherty et al., 1997). Thus, we think that the death of β5t-deficient mice infected with influenza virus is a result of incompetent CTL responses in the mice due to an altered repertoire of $CD8^+$ T cells.

Based on the analysis of mice expressing B cell lymphoma-derived single MHC peptides, it was previously assumed that any peptide that causes low-avidity TCR engagement can trigger positive selection of thymocytes and that rather than positive selection, subsequent negative selection establishes repertoire formation of T cells (Ignatowicz et al., 1996; Huseby et al., 2005). It was additionally shown that the ability to induce positive selection experimentally was not limited to cTECs but also included fibroblasts and T-lineage cells (Pawlowski et al., 1993; Hugo et al., 1993; Zinkernagel and Althage, 1999; Martinic et al., 2003; Choi et al., 2005; Li et al., 2005). In fact, if positive selection should select developmental thymocytes solely according to low-avidity TCR engagement, any MHC-peptide complex expressed by any cell type could support the generation of a full repertoire of T cells. However, our results demonstrate that the development of an immunocompetent T cell repertoire requires positive selection by thymoproteasome-dependent MHC class I -peptide complexes specifically expressed by cTECs. Thus, the small number and unusual repertoire of T cells positively selected by the single MHC-peptides (Ignatowicz et al., 1996; Fukui et al., 1997) may resemble abnormal positive selection and incompetent T cell development detectable in β5t-deficient mice. Accordingly, similar to β5t-deficient cTECs, fibroblasts and hematopoietic cells can only induce positive selection of only a limited repertoire of T cells, such as 2C-TCR-transgenic T cells, but not HY-TCR-transgenic T cells (Zerrahn et al., 1999; Lilić et al., 2002). Instead, our results support the idea that self-peptides expressed by cTECs critically contribute to the establishment of an immunocompetent T cell repertoire (Singer et al., 1986).

The unique peptide-producing activity of cTECs may not be limited to MHC class I-associated peptides but also occur in MHC class II -associated peptides (Takahama et al., 2008), since cathepsin L and thymus-specific serine protease, which are lysosomal proteases that are highly expressed by cTECs, are required for the optimal generation of the CD4 T cell repertoire